

Azimuthal correlation in DIS*

A. Banfi, G. Marchesini, G. Smye

*Dipartimento di Fisica, Università di Milano-Bicocca and
INFN, Sezione di Milano, Italy*

ABSTRACT: We introduce the azimuthal correlation for the deep inelastic scattering process. We present the QCD prediction to the level of next-to-leading log resummation, matching to the fixed order prediction. We also estimate the leading non-perturbative power correction. The observable is compared with the energy-energy correlation in e^+e^- annihilation, on which it is modelled. The effects of the resummation and of the leading power correction are both quite large. It would therefore be particularly instructive to study this observable experimentally.

KEYWORDS: QCD, Deep Inelastic Scattering, Jets, Nonperturbative Effects.

*Research supported in part by the EU Fourth Framework Programme, ‘Training and Mobility of Researchers’, Network ‘Quantum Chromodynamics and the Deep Structure of Elementary Particles’, contract FMRX-CT98-0194 (DG12 - MIHT).

Contents

1. Introduction	2
2. QCD description	4
2.1 Elementary hard process	4
2.2 The observable at parton level	5
3. Resummation	7
4. The result	10
4.1 Hard contribution	10
4.2 Full contribution	12
5. Numerical evaluation	15
6. Discussion	17
A. Elementary partonic cross-sections	19
B. Observable decomposition	21
C. DL approximation	22
C.1 Large b (soft) contribution	23
C.2 Small b (hard) contribution	23
C.3 Comparison with EEC	24
D. Soft contribution	25
D.1 Dipoles 12 and 13	25
D.2 Dipole 23	26
D.3 NP contribution	27
E. Estimates of $\langle b \rangle$ using 1-loop coupling	29
F. Formulæ for numerical analysis	30

1. Introduction

One of the first observables studied in QCD was the energy-energy correlation (EEC) in e^+e^- annihilation [1, 2, 3]. It is a function of θ , the polar angle between pairs of hadrons weighted by their energy. A similar correlation in DIS involves not a polar but an azimuthal angle. Here the observable is given by

$$H(\chi) = \sin \chi \sum_{hh'} \frac{p_{th} p_{th'}}{Q^2} \delta(\cos \chi + \cos \phi_{hh'}), \quad \phi_{hh'} = \phi_h - \phi_{h'}, \quad 0 \leq \chi \leq \pi, \quad (1.1)$$

where the sum runs over all outgoing hadron pairs with p_{th} and ϕ_h the transverse momentum and azimuthal angle in the Breit frame. We take $-\pi < \phi_{hh'} \leq \pi$. The distribution for the observable $H(\chi)$ is dominated by events with large p_t jets: indeed we wish to exclude events with p_t much less than Q in order that we can perform the calculation based on a dijet type configuration. On the other hand, to simplify the QCD analysis and consider the incoming γ or Z_0 as pointlike, one should limit the distribution to events in which all jet p_t are not much larger than Q . A convenient¹ way to set these conditions is obtained by limiting the dijet resolution variable y_2 defined by the k_t jet finding algorithm [4] as follows:

$$y_- < y_2 < y_+. \quad (1.2)$$

Here the lower bound y_- selects large p_t events, while the upper bound y_+ allows us to consider the incoming vector boson as pointlike.

The azimuthal differential distribution for this observable is then defined, at fixed x_B and Q^2 , by

$$\frac{d\sigma(\chi, y_{\pm})}{d\chi dx_B dQ^2} = \sum_n \int \frac{d\sigma_n}{dx_B dQ^2} \Theta(y_+ - y_2) \Theta(y_2 - y_-) \cdot H(\chi), \quad (1.3)$$

with $d\sigma_n/dx_B dQ^2$ the distribution for n emitted hadrons in the process under consideration. One introduces the following normalized azimuthal correlation (E_TE_TC)

$$\begin{aligned} \frac{d\Sigma(\chi, y_{\pm})}{d\chi} &= \sigma^{-1}(y_{\pm}) \frac{d\sigma(\chi, y_{\pm})}{d\chi dx_B dQ^2}, \\ \sigma(y_{\pm}) &= \sum_n \int \frac{d\sigma_n}{dx_B dQ^2} \Theta(y_+ - y_2) \Theta(y_2 - y_-) \left(\sum_{h=1}^n \frac{p_{th}}{Q} \right)^2. \end{aligned} \quad (1.4)$$

By taking into account the case $h = h'$ in (1.1), i.e. $\chi = \pi$, this correlation is normalized to 1. We will be concerned with the back-to-back region of small $\chi = \pi - |\phi|$.

¹This method to set a limit on the large transverse momenta should contain small hadronization corrections, see [5, 6, 7].

A standard method to start to understand the behaviour of this correlation for small χ consists in trying to exponentiate the leading logarithmic one-loop contribution given² by

$$\Sigma(\chi, y_{\pm}) = 1 - C_T \frac{\alpha_s}{4\pi} \ln^2 \frac{1}{\chi^2} + \dots, \quad C_T = 2C_F + C_A, \quad \chi \ll 1, \quad (1.5)$$

where C_T is the total colour charge of the three hard partons $q\bar{q}g$ generating both the outgoing dijet and the incoming proton jet. The exponentiation of this one-loop term gives a characteristic Sudakov form factor leading to an azimuthal differential distribution $d\Sigma/d\chi$ with a peak at small χ near

$$\chi \sim e^{-\pi/(2C_T\alpha_s)}. \quad (1.6)$$

This is actually what happens for EEC in e^+e^- annihilation in the back-to-back region (small $\chi = \pi - |\theta|$ with θ the polar angle): the leading logarithmic one-loop contribution of $\Sigma_{e^+e^-}(\chi)$, is given by the same expression in (1.5) with $C_T = 2C_F$, the charge of the $q\bar{q}$ pair in the hard vertex. In this case the complete QCD analysis [1, 2, 3] and the data [8] confirm the presence in $d\Sigma_{e^+e^-}/d\chi$ of the Sudakov peak in (1.6).

There are experimental indications that azimuthal distributions behave differently. For instance, in $p\bar{p}$ processes, the differential distribution in the azimuthal angle between two hadrons behaves smoothly in the back-to-back region and shows no sign of a peak, as reported for instance in [9]. We should then understand why $E_T E_T C$ and EEC behave differently.

In this paper we perform the QCD analysis of the DIS azimuthal correlation (1.4) in the back-to-back region. The analysis is similar to the one [1, 2, 3] for EEC with a few major differences:

- the distribution (1.4) is dominated by dijet events which originate from the $q\bar{q}g$ hard system (3-jet events including the beam). Only recently has the QCD analysis been extended to distributions involving 3 jets [6, 7, 10] at the same accuracy as available in the study of 2-jet CIS distributions [11, 12];
- the radiation off the incoming parton contributes not only to the observable $H(\chi)$, but also to the parton density evolution;
- QCD resummation is performed in the 1-dimensional impact parameter b conjugate to the azimuthal angle. In the EEC case the variable is a polar angle and then one deals with the standard 2-dimensional impact parameter.

As in other similar analyses, see [7, 10, 12], due to QCD coherence, the radiation factorizes giving rise to the evolved standard parton density functions times the “radiation factor”, a collinear and infrared safe (CIS) quantity involving 3-jet emission;

²Contributions from parton density functions in $E_T E_T C$ enter beyond double logarithmic level.

We work at the following accuracy: (i) double (DL) and single (SL) logarithmic perturbative (PT) resummation (for the logarithm of the distribution in the b -representation we resum all terms $\alpha_s^n \ln^{n+1} bQ$ and $\alpha_s^n \ln^n bQ$); (ii) matching of resummed with exact fixed order results (in this paper only to one-loop order); (iii) leading non-perturbative (NP) corrections coming from the fact that the QCD coupling runs into the infrared region [5, 13].

The paper is organized as follows. In section 2 we discuss the QCD process and the observable $H(\chi)$. In section 3 we describe the procedure for the resummation at SL level. In section 4 we present the result of the resummation and evaluate the leading power correction. In section 5 we present the numerical evaluation. In section 6 we summarize and discuss our result. Appendices contain the technical details.

2. QCD description

We work in the Breit frame of the DIS process with P and q the momenta of the incoming proton and the exchanged vector boson (γ or Z_0)

$$q = \frac{Q}{2}(0, 0, 0, 2), \quad P = \frac{Q}{2x_B}(1, 0, 0, -1), \quad x_B = \frac{Q^2}{2(Pq)}. \quad (2.1)$$

We first discuss the QCD hard elementary vertex and then the secondary parton emission.

2.1 Elementary hard process

DIS dijet events originate from the elementary hard vertex

$$q P_1 \rightarrow P_2 P_3, \quad (2.2)$$

with P_1 along the z -axis. We take P_2, P_3 in the $\{y, z\}$ -plane, the “event-plane”, see appendix A. We use the kinematical variables

$$\xi = \frac{(P_1 P_2)}{(P_1 q)}, \quad x = \frac{Q^2}{2(P_1 q)} > x_B. \quad (2.3)$$

The outgoing transverse momentum P_t and the squared invariant masses $Q_{ab}^2 = 2(P_a P_b)$ are given by

$$P_t = Q \sqrt{\xi(1-\xi) \frac{1-x}{x}}, \quad Q_{12}^2 = \frac{\xi}{x} Q^2, \quad Q_{13}^2 = \frac{1-\xi}{x} Q^2, \quad Q_{23}^2 = \frac{1-x}{x} Q^2. \quad (2.4)$$

We distinguish P_2 from P_3 by assuming

$$(P_1 P_2) < (P_1 P_3), \quad (2.5)$$

which restricts us to the region $0 < \xi < \frac{1}{2}$. In appendix A we report the elementary distributions for the process (2.2) as functions ξ and x . They depend on the “configurations” of the three partons. If we consider only photon exchange it is enough to identify the gluon momentum, we use the index $\delta = 1, 2$ or 3 to denote that the gluon momentum is P_1, P_2 or P_3 respectively. If we consider also Z_0 exchange, with parity-violating terms, we need to identify also the nature of incoming parton, this will be identified by the index $\tau = q, \bar{q}, g$. Finally for quarks we need to introduce also the flavour index f . The configuration of the hard vertex will be then defined by the configuration index $\rho = \{\delta, \tau, f\}$, see appendix A for a detailed presentation of these conventions.

2.2 The observable at parton level

The QCD process involving multi-parton emission is described by one incoming parton of momentum p_1 (inside the proton) and two outgoing hard partons p_2, p_3 accompanied by an ensemble of secondary partons k_i

$$q p_1 \rightarrow p_2 p_3 k_1 \cdots k_n, \quad p_1 = x_1 P. \quad (2.6)$$

Here, taking a small subtraction scale μ (smaller than any other scale in the problem), we have assumed that p_1 (and the spectators) are parallel to the incoming proton.

Since $H(\chi)$ in (1.1) is linear in p_h and $p_{h'}$ we may replace the sum over hadrons with a sum over outgoing partons for the process (2.6). To compute the distribution for small χ at SL accuracy, we can consider the secondary partons to be soft and take the contributions to $H(\chi)$ up to the first linear correction in the soft limit. Hard collinear radiation in the jets gets embodied into the hard scale of the corresponding radiator, see [11], and, in the case of the incoming jet, contributes to the parton density function, see [7, 10, 12]. In this limit the outgoing hard partons p_2 and p_3 tend to P_2 and P_3 , with soft recoil we need to consider to first order. From appendix B, we have

$$p_{t2} p_{t3} \simeq P_t^2 \left(1 - \sum_i \frac{|k_{yi}|}{P_t} \right), \quad \chi_{23} = \pi - |\phi_{23}| \simeq |\phi_x|, \quad \phi_x = \sum_i \frac{k_{xi}}{P_t}, \quad (2.7)$$

with k_{xi} the out-of-event-plane momentum component. The event plane is defined in appendix B and P_t in (2.4). Neglecting contributions to $H(\chi)$ from two secondary soft partons we have (see figure 1)

$$H(\chi) \simeq \frac{2P_t^2}{Q^2} \left\{ \left(1 - \sum_i \frac{|k_{yi}|}{P_t} \right) \delta(\chi - \chi_{23}) + \sum_i \frac{k_{ti}}{P_t} [\delta(\chi - \chi_{2i}) + \delta(\chi - \chi_{3i})] \right\}. \quad (2.8)$$

From the expression of $\chi_{ai} = \pi - |\phi_{ai}|$ we obtain in the soft limit (see appendix B)

$$[\delta(\chi - \chi_{2i}) + \delta(\chi - \chi_{3i})] \simeq \delta(\chi - |\bar{\phi}_i - \phi_x|), \quad |k_{yi}| \simeq k_{ti} |\cos \bar{\phi}_i|, \quad (2.9)$$

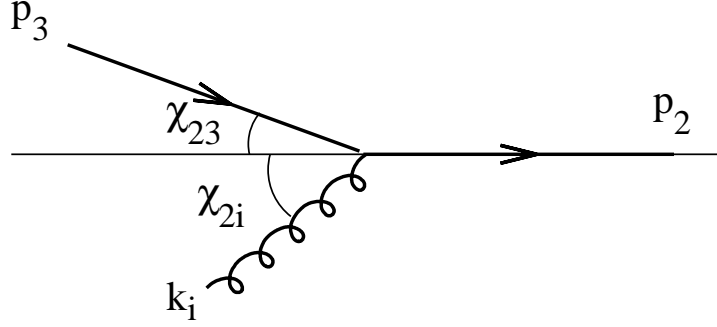


Figure 1: The kinematics of azimuthal correlation in the plane orthogonal to the Breit axis. The hard partons p_2 and p_3 correspond to the configuration $\delta = 1$ and k_i is a soft secondary gluon.

with $\bar{\phi}_i$ the azimuthal angle between k_i and either the hard parton p_2 or p_3 :

$$\bar{\phi}_i = \begin{cases} \phi_{i2} & \text{for } k_i \text{ near } p_2, \\ \phi_{3i} & \text{for } k_i \text{ near } p_3. \end{cases} \quad (2.10)$$

Splitting the expression of $H(\chi)$ into a ‘hard’ and a ‘soft’ contribution we can write, to first order in softness,

$$H(\chi) \simeq H_h(\chi) + H_s(\chi), \quad (2.11)$$

where,

$$\begin{aligned} H_h(\chi) &= \frac{2P_t^2}{Q^2} \delta(\chi - |\phi_x|), \\ H_s(\chi) &= \frac{2P_t^2}{Q^2} \sum_i \frac{k_{ti}}{P_t} [\delta(\chi - |\bar{\phi}_i - \phi_x|) - |\cos \bar{\phi}_i| \delta(\chi - |\phi_x|)]. \end{aligned} \quad (2.12)$$

This form explicitly shows that $H(\chi)$ is, by itself, a CIS observable in the sense that the azimuthal correlation has nothing more than the singularities of the total DIS cross section, namely the incoming parton collinear singularities leading to the anomalous dimension, see later. Indeed, the hard term H_h (hard-hard contribution with no recoil, $p_{t2}p_{t3} \rightarrow P_t^2$) depends only on the total recoil $|\phi_x|$ from secondary partons. The soft term H_s (hard-soft contribution together with the recoil piece of hard-hard contribution) is present only in the real contribution. Here the *soft* singularity of the matrix element is damped by the k_{ti} factor, while the *collinear* singularity, $\bar{\phi}_i \rightarrow 0$, is regularised by the vanishing difference of the delta functions in the square brackets.

3. Resummation

Considering the region $\chi \ll 1$, the starting point for the QCD resummation of the azimuthal distribution is the factorization [14] of the square amplitude for the process (2.6) with n secondary partons soft or collinear to the primary partons P_a in the hard vertex (2.2). For each configuration ρ we have

$$|M_n(k_1 \dots k_n)|^2 \simeq |M_0|^2 \cdot S_n(k_1 \dots k_n). \quad (3.1)$$

The first factor is the squared amplitude for the elementary vertex (2.2) for the different configurations ρ . It gives rise to the elementary hard distribution $d\hat{\sigma}_\rho$ as function of the kinematical variables x and ξ in (2.3), see appendix A. The second factor is the distribution of secondary partons emitted from the hard momenta P_a . Since in the emission, the nature of incoming parton changes, S_n is a matrix in the configuration index ρ . Corrections to the factorized expression are relevant for finite χ and can be taken into account by a non-logarithmic coefficient function. From (3.1) the azimuthal correlation (1.3) is then given by

$$\frac{d\sigma(\chi, y_\pm)}{d\chi dx_B dQ^2} = \sum_\rho \int_{x_B}^{x_M} \frac{dx}{x} \int_{\xi_-}^{\xi_+} d\xi \left(\frac{d\hat{\sigma}_\rho}{dx d\xi dQ^2} \right) C_\rho(\alpha_s) \cdot \mathcal{I}_\rho(\chi; Q_{ab}), \quad (3.2)$$

where the limits x_M, ξ_\pm are determined by the values of y_\pm which limit the transverse momenta, see appendix A. Here $C_\rho(\alpha_s)$ is the non-logarithmic coefficient function

$$C_\rho(\alpha_s) = 1 + \frac{\alpha_s}{\pi} c_1^{(\rho)}(\chi) + \mathcal{O}(\alpha_s^2). \quad (3.3)$$

The distribution \mathcal{I} depends on the geometry of the dijet system through the hard scales Q_{ab} given in (2.4). It is given by

$$\mathcal{I}(\chi) = \int_0^1 dx_1 \mathcal{P}(x_1, \mu) \sum_n \frac{1}{n!} \int d\Gamma_n \cdot S_n(k_1 \dots k_n), \quad (3.4)$$

where $\mathcal{P}(x_1, \mu)$ are the parton density functions at the (small) subtraction scale μ and x_1 is the incoming parton momentum fraction (2.6). The phase space and observable are contained in

$$d\Gamma_n = \prod_{i=1}^n \int \frac{d^3 k_i}{\pi \omega_i} \cdot \{H_h(\chi) + H_s(\chi)\} \cdot \delta \left(\frac{x_B}{x} - x_1 \prod_{i \in \mathcal{C}_1} z_i \right). \quad (3.5)$$

The last delta function accounts for the fact that the incoming parton p_1 loses energy by radiation. Here z_i is the collinear splitting energy fractions for radiation of secondary partons k_i in the region \mathcal{C}_1 collinear to p_1 . Note that it is this last delta function which is responsible for the non cancellation of the (residual) incoming parton collinear singularities which build up the parton density function.

The resummation of the distribution \mathcal{I} is based on the factorization of soft and collinear contributions in S_n . Then one needs to factorize also the expression of $d\Gamma_n$. For the observable $H(\chi)$ this is done by 1-dimensional Fourier transform and, for the delta function in x_B , by Mellin transform

$$\begin{aligned} H_h(\chi) &= \frac{2P_t^2}{Q^2} \int_{-\infty}^{\infty} \frac{P_t db}{\pi} \cos(b\chi P_t) \prod_i e^{ibk_{xi}} , \\ H_s(\chi) &= \frac{2P_t^2}{Q^2} \int_{-\infty}^{\infty} \frac{P_t db}{\pi} \cos(b\chi P_t) \prod_i e^{ibk_{xi}} \left\{ \sum_j \frac{k_{tj}}{P_t} \left(e^{-iP_t b \bar{\phi}_j} - |\cos \bar{\phi}_j| \right) \right\} , \\ \delta \left(\frac{x_B}{x} - x_1 \prod_{i \in \mathcal{C}_1} z_i \right) &= \frac{1}{x_1} \int \frac{dN}{2\pi i} \left(\frac{x_B}{xx_1} \right)^{-N} \prod_i \epsilon(z_i) , \end{aligned} \quad (3.6)$$

where the last integral runs parallel to the imaginary axis with $\text{Re}(N) > 1$ and

$$\epsilon(z_i) = z_i^{N-1}, \text{ for } k_i \in \mathcal{C}_1, \quad \epsilon(z_i) = 1, \text{ for } k_i \notin \mathcal{C}_1. \quad (3.7)$$

Each secondary parton contributes to $d\Gamma_n$ by a factor

$$[\epsilon(z_i) \cos(bk_{xi}) - 1] = [\epsilon(z_i) - 1] \cos(bk_{xi}) - [1 - \cos(bk_{xi})], \quad (3.8)$$

with the one included to take into account virtual corrections. Since S_n is even in all k_{xi} , we have replaced $e^{ibk_{xi}} \rightarrow \cos(bk_{xi})$.

The splitting made in (3.8) shows that we can resum independently the parton density function and the radiation function of the observable H . Indeed, from the well known SL approximation

$$[1 - \cos(bk_{xi})] \simeq \Theta(|k_{xi}| - \bar{b}^{-1}), \quad \bar{b} = e^{\gamma_E} |b|, \quad (3.9)$$

we have that the first term in (3.8) involves partons in the region $k_{xi} \lesssim \bar{b}^{-1}$ collinear to P_1 with weight $[z_i^{N-1} - 1]$. Their contributions reproduce the anomalous dimension and resum to the parton density function at the proper hard scale which is \bar{b}^{-1} . The second term in (3.8) involves partons in the complementary region with weight -1 , only virtual contributions survive. Their contributions are resummed to give the standard radiation factor for the observable $H(\chi)$ with (virtual) frequencies larger than \bar{b}^{-1} . This method to show the factorization of these two contributions has been used and discussed in [7, 10, 12].

The final result for \mathcal{I} thus becomes

$$\mathcal{I}_{\tau, \delta, f}(\chi; Q_{ab}) = \frac{4P_t^2}{Q^2} \int_0^\infty \frac{P_t db}{\pi} \cos(b\chi P_t) \cdot \mathcal{P}_{\tau, f} \left(\frac{x_B}{x}, \bar{b}^{-1} \right) \cdot \mathcal{A}_\delta(b; Q_{ab}), \quad (3.10)$$

where the radiation factor is given by the sum of the hard and the soft contribution

$$\mathcal{A}_\delta(b) = \mathcal{A}_\delta^h(b) + \mathcal{A}_\delta^s(b), \quad \mathcal{A}_\delta^h(b) = e^{-\mathcal{R}_\delta(b)}, \quad \mathcal{A}_\delta^s(b) = e^{-\mathcal{R}_\delta(b)} \cdot B_\delta(b). \quad (3.11)$$

It will be seen that only the hard contribution is required for a PT resummation at SL level, while the soft contribution is responsible for leading NP corrections.

Here \mathcal{R}_δ is the full CIS radiator for the secondary emission and is given by

$$\mathcal{R}_\delta(b) = \int \frac{d^3k}{\pi\omega} W_\delta(k) [1 - \cos(bk_x)] . \quad (3.12)$$

The quantity B_δ , representing the $H_s(\chi)$ contribution to the observable, is

$$B_\delta(b) = \int \frac{d^3k}{\pi\omega} W_\delta(k) \frac{k_t}{P_t} [\cos(bP_t\bar{\phi}) - |\cos\bar{\phi}|] . \quad (3.13)$$

Here $W_\delta(k)$ is the two-loop distribution for the emission of the soft gluon from the primary three hard partons P_a in the configuration δ :

$$W_\delta(k) = \frac{N_c}{2} \left(w_{\delta a} + w_{\delta b} - \frac{1}{N_c^2} w_{ab} \right) , \quad a \neq b \neq \delta , \quad (3.14)$$

where $w_{ab}(k)$ is the standard distribution for emission of a soft gluon from the ab -dipole. It has a simple expression in the ab -dipole centre of mass. Representing in this frame the soft gluon momentum by Sudakov decomposition

$$k^* = \alpha P_a^* + \beta P_b^* + \kappa , \quad \alpha\beta = \frac{\kappa^2}{Q_{ab}^2} , \quad (3.15)$$

with P_a^* and P_b^* back-to-back momenta ($Q_{ab}^2 = 2P_a^*P_b^*$) and κ a two-dimensional transverse vector, we can write

$$w_{ab}(k) = \frac{\alpha_s(\kappa)}{\pi\kappa^2} , \quad \frac{d^3k}{\pi\omega} = \frac{d^2\kappa}{\pi} \frac{d\alpha}{\alpha} , \quad \alpha > \frac{\kappa^2}{Q_{ab}^2} . \quad (3.16)$$

To ensure SL accuracy, we have to take α_s defined in the physical scheme [15]. Taking P_a^*, P_b^* along the z -axis, the x -components of the momenta are the same as the ones in the laboratory frame with the event plane given by the yz -plane. We then have $k_x = \kappa_x$.

A similar analysis gives the (weighted) total cross section $\sigma(y_\pm)$ in (1.4) needed to obtain the normalized differential distribution $d\Sigma(\chi)/d\chi$. We find

$$\sigma(y_\pm) = \sum_\rho \int_{x_B}^{x_M} \frac{dx}{x} \int_{\xi_-}^{\xi_+} d\xi \left(\frac{d\hat{\sigma}_\rho}{dx d\xi dQ^2} \right) \frac{4P_t^2}{Q^2} \mathcal{P}_\rho \left(\frac{x_B}{x}, Q \right) , \quad (3.17)$$

where the parton density function is reconstructed at the unconstrained DIS hard scale Q .

In conclusion we have that, while in the DIS cross section the proper hard scale of the parton density functions is Q , in the distribution (3.10) it is given by \bar{b}^{-1} . This is a result of QCD coherence.

4. The result

The general structure in (3.11) of the radiation factor is similar to the one in EEC: the hard term \mathcal{A}_δ^h gives the PT contribution at SL accuracy. The soft term \mathcal{A}_δ^s is beyond SL accuracy. On the contrary, for the NP correction, it is the soft term which gives the leading $1/Q$ -power piece; the hard term gives a subleading $1/Q^2$ piece. We discuss these results in the two next subsections.

4.1 Hard contribution

We start from the PT part of the radiator (3.12) which is given at SL accuracy by the approximation (3.9). This has been computed in [7] (where it corresponds to the replacements $\nu \rightarrow 0$ and $\nu\beta_2, \nu\beta_3 \rightarrow b$). We have

$$\mathcal{R}_\delta^{\text{PT}}(b) = R_\delta(b) = \sum_{a=1}^3 C_a^{(\delta)} r(\bar{b}, \zeta_a^{(\delta)} Q_a^{(\delta)}) , \quad r(\bar{b}, Q) = \int_{1/\bar{b}}^Q \frac{dk}{k} \frac{2\alpha_s(2k)}{\pi} \ln \frac{Q}{2k} , \quad (4.1)$$

where the various hard scales and constants are, see [7, 10],

$$\begin{aligned} Q_a^{(\delta)} &= Q_b^{(\delta)} = Q_{ab} , & C_a^{(\delta)} &= C_b^{(\delta)} = C_F , & \zeta_a^{(\delta)} &= \zeta_b^{(\delta)} = e^{-\frac{3}{4}} , \\ Q_\delta^{(\delta)} &= \frac{Q_{a\delta} Q_{\delta b}}{Q_{ab}} , & C_\delta^{(\delta)} &= C_A , & \zeta_\delta^{(\delta)} &= e^{-\frac{\beta_0}{4N_c}} , \end{aligned} \quad (4.2)$$

with δ a gluon and a or b a quark (or antiquark), β_0 is the first coefficient of the beta function (see (D.24)). As is typical for a 3-jet quantity, the scale for the quark or antiquark terms of the radiator is the $q\bar{q}$ invariant mass, while the scale for the gluon term is given by the gluon transverse momentum with respect to the $q\bar{q}$ system. The rescaling factors $\zeta_a^{(\delta)}$ take into account SL contributions from non-soft secondary partons collinear to the primary partons P_a . The integration variable k in (4.1) is the out-of-plane component of momentum k_x and α_s is taken in the physical scheme [15]. The rescaling factor 2 in the running coupling comes from the integration over the in-plane momentum component. The exact expression of hard scales and of rescaling factors in (4.2) is relevant at SL level.

The complete SL resummed result is then given by

$$\frac{d\Sigma^{\text{PT}}(\chi, y_\pm)}{d\chi} = \sigma^{-1}(y_\pm) \sum_\rho \int_{x_B}^{x_M} \frac{dx}{x} \int_{\xi_-}^{\xi_+} d\xi \left(\frac{d\hat{\sigma}_\rho}{dx d\xi dQ^2} \right) C_\delta(\alpha_s) \cdot \mathcal{I}_\rho^{\text{PT}}(\chi) , \quad (4.3)$$

where

$$\mathcal{I}_\rho^{\text{PT}}(\chi) = \int_0^\infty \frac{P_t db}{\pi} \cos(b\chi P_t) \mathcal{F}_\rho(b) , \quad \mathcal{F}_\rho(b) \equiv \frac{4P_t^2}{Q^2} \mathcal{P}_{\tau,f} \left(\frac{x_B}{x}, \bar{b}^{-1} \right) e^{-R_\delta(b)} . \quad (4.4)$$

The integrand is computed at SL accuracy in b -space, that is, $\ln \mathcal{F}_\rho(b)$ resums all terms $\alpha_s^n \ln^{n+1} bQ$ and $\alpha_s^n \ln^n bQ$. For $\chi \rightarrow 0$ we have that $\mathcal{I}^{\text{PT}}(0)$ has a $1/\sqrt{\alpha_s}$ -singular behaviour (it is essentially given by the integral of a Sudakov form factor,

see [2] for the EEC case). Formally the upper limit of b -integration is set to infinity, but actually, from (4.1) is $\bar{b} < 2/\Lambda_{\text{QCD}}$.

As we shall see, the differential azimuthal distribution is monotonically decreasing by increasing χ . This is in contrast with the EEC case in which the differential distribution (analogous to $d\Sigma(\chi)/d\chi$) develops a peak in the small χ region (the back-to-back polar angle in this case), which is present also in the data (see [8]). In the next section we present the numerical evaluation of the azimuthal distribution while for the remainder of this section we discuss the origin of this behaviour and of the differences with respect to the EEC case.

General features To discuss $\mathcal{I}^{\text{PT}}(\chi)$ for small χ (index δ neglected here) we divide the b -integral at the point $b_0 = 1/(\bar{\chi}P_t)$ with $\bar{\chi} = \chi e^{\gamma_E}$:

$$\mathcal{I}^{(-)}(\chi) = \frac{d}{d\chi} \int_0^{b_0} \frac{db}{\pi b} \sin(\chi b P_t) \mathcal{F}(b), \quad \mathcal{I}^{(+)}(\chi) = \frac{d}{d\chi} \int_{b_0}^{\infty} \frac{db}{\pi b} \sin(\chi b P_t) \mathcal{F}(b). \quad (4.5)$$

The sine function oscillates with a first maximum above the splitting point. The integrand $\mathcal{F}(b)$ has a Sudakov behaviour at large b (see in appendix C the discussion for \mathcal{F} in DL approximation). From this behaviour we have that the two contributions behave as follows:

- $\mathcal{I}^{(+)}(\chi)$ is dominated by the lower bound at $b = b_0$

$$\mathcal{I}^{(+)}(\chi) \simeq \frac{e^{-R(1/\bar{\chi}P_t)}}{\chi} \cdot \mathcal{S}^{(+)}(\chi), \quad (4.6)$$

where, for small χ , the remainder $\mathcal{S}^{(+)}(\chi)$ can be expanded in the SL function

$$R'(\chi) = 2C_T \frac{\alpha_s}{\pi} \ln \frac{1}{\chi}, \quad C_T = 2C_F + C_A. \quad (4.7)$$

The Sudakov factor e^{-R}/χ in (4.6) has a peak at $\chi \sim \chi_1$ with $R'(\chi_1) = 1$ which corresponds to (1.6). This Sudakov behaviour is expected since large values of b force all the emitted k_{xi} to be soft, $|k_{xi}| \lesssim \chi P_t$.

- $\mathcal{I}^{(-)}(\chi)$ takes contributions from values of b not necessarily large. It is a decreasing function of χ from the value $\mathcal{I}^{(-)}(0)$ and has a $1/\sqrt{\alpha_s}$ -singular behaviour. For b not large, the soft recoil $\chi P_t = |\sum_i k_{xi}|$ is obtained by cancellations among some larger k_{xi} .

The relative size of the two contributions in (4.5) can be estimated by the DL approximation of \mathcal{F} , see appendix C. One finds that the two terms $\mathcal{I}^{(\pm)}(\chi)$ become comparable at $\chi \sim \chi_1$, i.e. just near the Sudakov peak and for smaller χ the contribution $\mathcal{I}^{(-)}(\chi)$ takes over. As a result, the differential azimuthal distribution $d\Sigma(\chi)/d\chi$ continuously decreases from $\chi = 0$ and does not have a peak at small χ .

Comparison with EEC. The behaviour of $d\Sigma_{e^+e^-}(\chi)/d\chi$, the differential EEC with χ the back-to-back polar angle in e^+e^- , is very different. This distribution is given by an expression similar to (4.4) with the most important difference³ being that in EEC the integration measure is χd^2b instead of db . As a consequence, the contribution involving the finite b regions, which corresponds to $\mathcal{I}^{(-)}(\chi)$ in (4.5), is relevant⁴ only for $\chi \ll \chi_1$ with χ_1 the position of the Sudakov peak given in (1.6) for $C_T = 2C_F$. Therefore, the distribution $d\Sigma_{e^+e^-}(\chi)/d\chi$ manifests a Sudakov behaviour in the small χ region. The fact that the contribution involving the finite b -region is essentially negligible in the EEC case can be argued by observing that it is dominated by emitted transverse momenta \vec{k}_{ti} not necessarily soft which have to sum up to a total soft recoil. The constraint of momentum cancellation in 2-dimension is much stronger than in 1-dimension as for the azimuthal case.

A similar way to see the different behaviour in the EEC and $E_T E_T C$ cases, is obtained by trying to factorize the Sudakov form factor e^{-R}/χ from the differential distribution. In the EEC case the remainder factor can be expressed in terms of the SL variable $R'(\chi)$ (with $C_T = 2C_F$) in the full range $\chi \gtrsim \chi_1^2$ (with χ_1 the position of the Sudakov peak). In the $E_T E_T C$ case instead the remainder factor is a function of $R'(\chi)$ only in the range $\chi \gtrsim \chi_1$ while at smaller χ it does cancel the e^{-R}/χ factor and then it is not any more a SL function, see in appendix C the analysis in the DL approximation.

4.2 Full contribution

To complete the analysis we need to take into account also \mathcal{A}_s^s in (3.11) corresponding to $H_s(\chi)$, the soft contribution to the observable, see (2.12). From (3.14) we can write

$$B_\delta(b) = \frac{N_c}{2} \left(B_{\delta a} + B_{\delta b} - \frac{1}{N_c^2} B_{ab} \right), \quad a \neq b \neq \delta, \quad (4.8)$$

with the $\{ab\}$ -dipole contribution given by

$$B_{ab}(b) = \int_0^{Q_{ab}} \frac{d^2\kappa}{\pi\kappa^2} \frac{\alpha_s(\kappa)}{\pi} \int_{\kappa^2/Q_{ab}^2}^1 \frac{d\alpha}{\alpha} \cdot \frac{k_t}{P_t} [\cos(bP_t\bar{\phi}) - |\cos\bar{\phi}|]. \quad (4.9)$$

Here the integration variables κ and α are the momentum components of the soft gluon in the $\{ab\}$ -dipole centre of mass (see (3.15) and (3.16)), while k_t and $\bar{\phi}$ are the transverse momentum and azimuthal angle in the Breit frame, see (2.10). In appendix D we give their kinematical relations. For instance, for the 12-dipole we

³In EEC case the integrand $\mathcal{F}(b)$ is simply given by the exponential of a radiator $R(b)$, which involves only two hard emitters, the $q\bar{q}$ pair with total charge $C_T = 2C_F$, and the cosine is replaced by the Bessel function.

⁴From the DL approximation this term becomes comparable to the large b -term, corresponding to $\mathcal{I}^{(+)}(\chi)$ in (4.5), at $\chi \sim \chi_2 = \chi_1^2$, i.e. $R'(\chi_2) = 2$. See [2].

have

$$k_y = \alpha P_t + \kappa_y, \quad \tan \bar{\phi} = \frac{\kappa_x}{\kappa_y}, \quad (4.10)$$

where we used the fact that the Lorentz transformations between the two frames do not involve the x -direction so that $k_x = \kappa_x$. The result (4.10) can be easily recovered for instance observing that for soft transverse momentum in the dipole frame $\kappa \rightarrow 0$, the momentum k becomes collinear to P_2 for $\alpha > 0$ and to P_1 for $\alpha \rightarrow 0$.

The two terms in the square brackets of (4.9) have DL singularities for $\kappa \rightarrow 0$ and $\bar{\phi} \rightarrow 0$. However the sum (multiplied by k_t) is regular which gives

$$\mathcal{A}_\delta^s(b) \sim \alpha_s \cdot \mathcal{A}_\delta^h(b), \quad (4.11)$$

so that this term contributes at PT level beyond SL accuracy, see appendix D and [3]. This fact is carefully explained at the end of section 2. Recall that the cancellation is between the contributions to the observable $H(\chi)$ from the recoil of the two outgoing hard partons $\{p_2 p_3\}$ and from a soft secondary and a hard parton $\{k_i p_{2/3}\}$.

The soft part of the radiation factor \mathcal{A}_δ^s gives instead the leading NP correction which is proportional to b , see also [3]. This NP correction comes from the region in which the soft gluon in B_{ab} is collinear to one of the outgoing hard partons P_2 or P_3 . For instance for the B_{12} radiator, where (4.10) holds, this region corresponds to

$$k_y \simeq \alpha P_t \gg \kappa_x, \quad (4.12)$$

which gives

$$k_t \simeq \alpha P_t, \quad \cos(b P_t \bar{\phi}) \simeq \cos \frac{b \kappa_x}{\alpha}, \quad \cos \bar{\phi} \simeq 1.$$

Changing variable $u = b|\kappa_x|/\alpha$, and taking in the integrand the leading piece for $\kappa \rightarrow 0$, the contribution to $B_{12}(b)$ from this region is

$$\delta B_{12}(b) = b \int \frac{d\kappa^2}{\kappa^2} \frac{\kappa \alpha_s(\kappa)}{\pi} \int_{-\pi}^{\pi} \frac{d\phi}{2\pi} |\cos \phi| \int_0^\infty \frac{du}{u^2} [\cos u - 1] = -b \cdot \int \frac{d\kappa^2}{\kappa^2} \frac{\kappa \alpha_s(\kappa)}{\pi}, \quad (4.13)$$

with the integration over the NP region of small κ . It is simple to see that the regions non-collinear to the outgoing hard parton P_2 (away from (4.12)) lead to contributions which are even in b and then give subleading NP corrections. A correction linear in b is non-local in the conjugate variable χ , see [3].

To complete the calculation of the leading NP correction we use the standard procedure extensively discussed in [3, 16]. First we need to extend the meaning of the running coupling into the large distance region. This can be done by following the approach [5] in which one uses the dispersive representation

$$\frac{\alpha_s(\kappa)}{\kappa^2} = \int_0^\infty dm^2 \frac{\alpha_{\text{eff}}(m^2)}{(\kappa^2 + m^2)^2}. \quad (4.14)$$

Moreover one needs to take into account the non fully inclusive character of the observable $H(\chi)$. This can be done in two steps, see [16]. One replaces the momentum κ of the emitted soft gluon by $\kappa \rightarrow \sqrt{\kappa^2 + m^2}$, with m the mass of the gluon decaying products. Then one multiplies the result by the Milan factor \mathcal{M} . Finally one obtains

$$\delta B_{12}(b) = -b \cdot \lambda^{\text{NP}}, \quad \lambda^{\text{NP}} = \frac{2\mathcal{M}}{\pi} \int dm \delta\alpha_{\text{eff}}(m^2), \quad (4.15)$$

with $\delta\alpha_{\text{eff}}$ the large distance contribution of the effective coupling. See appendix D for the connection of λ^{NP} with the NP parameter already measured in 2-jet observables.

Similar leading NP corrections are obtained for the B_{13} and B_{23} pieces. Since they come from the phase space regions collinear to the outgoing hard partons P_2 and P_3 , the complete NP correction from (4.8) is proportional to the total charge of the hard outgoing primary partons

$$\delta B_\delta(b) = -\left(C_2^{(\delta)} + C_3^{(\delta)}\right) b \cdot \lambda^{\text{NP}}. \quad (4.16)$$

In the present analysis we concentrate on the leading power correction discussed above. Large angle emissions and the ones collinear to the incoming parton generate next-to-leading NP corrections, proportional to $b^2 \sim Q^{-2}$. They appear not only in this B term, but also in the radiator \mathcal{R} (see (3.12)) and in the parton density functions \mathcal{P} (see [5]). A complete study of higher orders NP corrections is still to be done.

The final answer for \mathcal{I} , including the leading NP correction in (4.16), thus is

$$\mathcal{I}_\rho(\chi; Q_{ab}) = \int_0^\infty \frac{P_t db}{\pi} \cos(b\chi P_t) \mathcal{F}_\rho(b) \cdot \left\{ 1 - \left(C_2^{(\delta)} + C_3^{(\delta)}\right) b \cdot \lambda^{\text{NP}} \right\}, \quad (4.17)$$

with $\mathcal{F}_\rho(b)$ the PT factor in (4.4). The final answer for the azimuthal correlation in (1.4) can be written in the form

$$\frac{d\Sigma(\chi, y_\pm)}{d\chi} = \frac{d\Sigma^{\text{PT}}(\chi, y_\pm)}{d\chi} \left\{ 1 - \lambda^{\text{NP}} \langle (C_2 + C_3) \cdot b \rangle \right\}, \quad (4.18)$$

with b (and the outgoing hard parton charges) averaged over the PT distribution in (4.4). One can give an estimation of $\langle b \rangle$ by using the one-loop coupling approximation. From appendix E we evaluate this mean at $\chi = 0$ and obtain

$$\langle b \rangle_{\chi=0} \sim \frac{1}{\Lambda_{\text{QCD}}} \left(\frac{\Lambda_{\text{QCD}}}{Q} \right)^\gamma, \quad \gamma = \frac{4}{\beta_0} C_T \ln \frac{2 + \frac{4}{\beta_0} C_T}{1 + \frac{4}{\beta_0} C_T} = 0.62 \quad (n_f=3). \quad (4.19)$$

Taking into account the two-loop coupling the exponent γ is not a constant but smoothly dependent on Q , see [3]. The detailed numerical analysis will be done in the next section.

5. Numerical evaluation

In the small χ region, the PT distribution is obtained from (4.3),(4.4) with the PT part of the radiator in (4.1). At larger values of χ one should use the exact PT result. In order to obtain a PT description valid for small and large χ one needs to match the resummed and the fixed order distribution. This amounts in computing, to the due order, the coefficient function $C_\delta(\alpha_s)$ in (3.3). This is usually done by comparing the resummed expression with the exact result.

We start from the integrated resummed distribution $\Sigma^{\text{PT}}(\chi)$ given by

$$\Sigma^{\text{PT}}(\chi) = \sigma^{-1}(y_\pm) \sum_\rho \int_{x_B}^{x_M} \frac{dx}{x} \int_{\xi_-}^{\xi_+} d\xi \left(\frac{d\hat{\sigma}_\rho}{dx d\xi dQ^2} \right) \int_0^\infty \frac{db}{\pi b} \sin(bP_t \chi) \mathcal{F}_\rho(b), \quad (5.1)$$

with $\mathcal{F}_\rho(b)$ the PT factor in (4.4) and $\sigma(y_\pm)$ the Born cross section (see (3.17)). In the following we describe in detail the adopted procedure for the first order matching using a fixed order numerical program such as [17, 18]. Notice that, in order to control the α_s scale, it is not sufficient to use first order matching but one needs to take into account also the two-loop analysis. To first order in α_s the resummed distribution $\Sigma^{\text{PT}}(\chi)$ in (5.1) reads

$$\Sigma^{\text{PT}}(\chi) = \frac{1}{2} \left(1 + \frac{\alpha_s}{2\pi} (G_{12}L^2 + G_{11}(y_\pm)L + c_1^{\text{res}}(y_\pm)) + \mathcal{O}(\alpha_s^2) \right), \quad L = -\ln \chi, \quad (5.2)$$

with $G_{12} = -2C_T$, G_{11} and c_1^{res} given in (F.5) and $\alpha_s = \alpha_{\overline{\text{MS}}}(Q)$. Here the factor 1/2 comes from the fact that the distribution (5.1) does not include the singular contribution proportional to $\delta(\chi - \pi)$. Only with this singular contribution the distribution is normalized to one.

Following [3], we match the resummed expression in (5.1) with the exact first order result $\Sigma_1(\chi)$, which is here obtained using the numerical program DISENT of ref. [17]. We obtain

$$\Sigma_{\text{mat}}^{\text{PT}}(\chi) = \frac{1}{2} + \left(1 + \frac{\alpha_s}{2\pi} (c_1 - c_1^{\text{res}}) \right) (\Sigma^{\text{PT}}(\chi) + \delta\Sigma(\chi)), \quad (5.3)$$

with $\Sigma^{\text{PT}}(\chi)$ the resummed distribution in (5.1), the coefficient

$$c_1 = \lim_{\chi \rightarrow 0} (\Sigma_1(\chi) - G_{12}L^2 - G_{11}L). \quad (5.4)$$

and the matching correction

$$\delta\Sigma(\chi) = \frac{1}{2} \left(\frac{\alpha_s}{2\pi} (\Sigma_1(\chi) - G_{12}L^2 - G_{11}L - c_1) \right). \quad (5.5)$$

Including the NP corrections we have:

$$\Sigma(\chi) = \frac{1}{2} + \left(1 + \frac{\alpha_s}{2\pi} (c_1 - c_1^{\text{res}}) \right) ((1 - \lambda^{\text{NP}} \langle (C_2 + C_3) \cdot b \rangle) \Sigma^{\text{PT}}(\chi) + \delta\Sigma(\chi)), \quad (5.6)$$

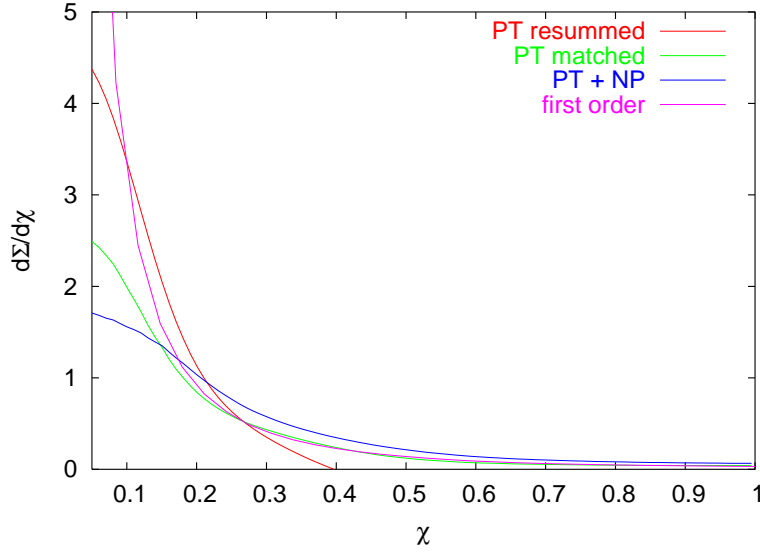


Figure 2: The azimuthal correlation distribution for $s = 98400 \text{ GeV}^2$, $x_B = 0.1$, $Q^2 = 900 \text{ GeV}^2$, $y_- = 1.0$ and $y_+ = 2.5$. The upper curve is the resummed PT distribution obtained from (5.1) (without matching), the lower curves are the PT and NP matched predictions obtained from (5.3) and (5.6) respectively. In the figure is also shown the first order prediction given by DISENT.

where b is now averaged over the PT integrated distribution in (5.1).

Here we report the result for the azimuthal correlation distribution with the following choices. We used the parton density function set MRST2001.1 [19] corresponding to $\alpha_s(M_Z) = 0.119$. We also set $\alpha_0(2 \text{ GeV}) = 0.52$ (see (D.23)), a value obtained from the analysis of two-jet event shapes [20].

In figure 2 we plot the full azimuthal distribution $d\Sigma/d\chi$ obtained from (5.6) for $x_B = 0.1$, $Q^2 = 900 \text{ GeV}^2$, $y_- = 1$ and $y_+ = 2.5$. The center of mass squared energy has been fixed at $s = 98400 \text{ GeV}^2$. In order to simplify the analysis (data are not yet available) we considered only the case of exchanged photon (see for instance the discussion in [7]).

Together with this curve we plot the fixed order PT distribution obtained from DISENT and the PT resummed distributions obtained from (5.1) and (5.3). We notice that the PT resummed curve follows the fixed order one for not too small values of χ . Then, while the first order starts developing a singularity for $\chi \rightarrow 0$, the resummed curve rises to a constant value. Actually the height of the ‘plateau’ is dramatically reduced after performing the first order matching. This is due to the large coefficient c_1 appearing in (5.3) ($c_1 \simeq -30$ in the present case).

The effect of the NP correction (5.6) is to further deplete the PT curve, in analogy with the EEC case [3].

6. Discussion

We presented the QCD analysis of $E_T E_T C$, the azimuthal correlation in DIS defined in (1.1)-(1.4). We considered small χ , the back-to-back azimuthal angle, and finite y_2 , the dijet resolution variable which selects dijet events and limits emitted jet transverse momenta not to exceed Q so that the exchanged photon is pointlike. This distribution is the generalization to DIS of EEC in e^+e^- .

The QCD resummation is performed in the 1-dimensional impact parameter b conjugate to the soft recoil $\chi P_t = |\sum_i k_{xi}|$, with k_{xi} the out-of-plane momenta of the undetected secondary partons, see (2.7). We sum all $\alpha_s^n \ln^{n+1} bQ$ and $\alpha_s^n \ln^n bQ$ terms in the exponent. The main complication with respect to the e^+e^- case is that $E_T E_T C$ involves also initial state radiation which contributes both to the incoming parton evolution and to the observable $H(\chi)$. Due to QCD coherence the two contributions factorize, see (3.10). We have indeed that $\bar{b}^{-1} \sim \chi P_t$ sets both the hard scale for the parton density functions \mathcal{P} (instead of Q as in the cross section, see (3.17)) and the lower limit to frequencies in “radiation factor” \mathcal{A} , a CIS quantity associated to the $q\bar{q}g$ hard vertex. See [7, 10, 12] for incoming radiation factorization in jet-shape observables in processes involving incoming hadrons.

For the PT result at SL accuracy one needs to consider only the hard term $H_h(\chi)$ of the observable from the two outgoing partons in the $q\bar{q}g$ hard system, see (2.12). The general behaviour of $d\Sigma^{\text{PT}}(\chi)/d\chi$ (and its comparison with EEC) can be simply explained by observing that there are essentially two phase space configurations for the secondary partons:

- all $|k_{xi}| \lesssim \chi P_t$. This gives a contribution to $d\Sigma^{\text{PT}}(\chi)/d\chi$ which behaves as a Sudakov form factor (4.6) with a peak at small χ , see (1.6);
- the other configurations, with some $|k_{xi}|$ exceeding the soft recoil. This corresponds to impact parameter with all values. Their contributions to $d\Sigma^{\text{PT}}(\chi)/d\chi$ lead to a $1/\sqrt{\alpha_s}$ -singular term (the integral of a Sudakov form factor) which is a decreasing function of χ starting from a finite value at $\chi = 0$, see appendix C.

The contributions from these two momentum configurations are comparable just at the Sudakov peak and for smaller χ the $1/\sqrt{\alpha_s}$ -singular term is dominating. As a result, $d\Sigma^{\text{PT}}(\chi)/d\chi$ is continuously decreasing with χ . Therefore the exponentiation of the one loop result in (1.5), with the characteristic Sudakov peak, is valid only above the Sudakov peak region. This is qualitatively different from the EEC behaviour in which the Sudakov peak is indeed manifest.

We have assumed [5, 13] that the leading power corrections are obtained when the argument of the QCD coupling runs into large distance regions. Such a hypothesis has been successfully tested in 2-jet shape observables [13] and EEC [3]. The azimuthal correlation (as other 3-jet observables [6, 7, 10]) provides a further way to explore this

assumption. Indeed, the running coupling enters our result with the three different arguments $\vec{\kappa}_{ab}$, the transverse momentum in the ab -dipole centre of mass frame. For each ab -dipole we evaluated the leading power corrections by taking $\kappa_{ab} \sim \Lambda_{\text{QCD}}$, thus obtaining the result (4.16). The three soft regions $\kappa_{ab} \sim \Lambda_{\text{QCD}}$ are very different. Consider for instance the leading power correction from the 12-dipole which is coming from the momentum region (see (4.12))

$$k_x = \kappa_x, \quad |k_y| \gg |\kappa_y| \sim |\kappa_x| \sim \Lambda_{\text{QCD}}, \quad (6.1)$$

where $\vec{\kappa} = \vec{\kappa}_{12}$ while \vec{k}_t is the transverse momentum in the Breit frame. We have that NP region $\kappa \sim \Lambda_{\text{QCD}}$ does not correspond to $k_t \sim \Lambda_{\text{QCD}}$. One finds analogous differences comparing $\vec{\kappa}_{12}$ with $\vec{\kappa}_{13}$ or $\vec{\kappa}_{23}$. This shows that analyzing $E_T E_T C$ (as well as 3-jet observables) we can further check whether NP corrections are controlled by the soft arguments in running coupling.

The strength of the leading power correction is controlled by the NP parameter λ^{NP} in (D.23) which is connected to the one in the thrust distribution, see (D.25). The leading power correction is similar to the ones in EEC: the expected $1/Q$ behaviour of the leading NP correction turns into $1/Q^\gamma$ with γ a slowly varying function of Q . We have $\gamma \simeq 0.62$ for three quark flavours, see (4.19).

In conclusion, this paper is a first step towards the full QCD analysis of azimuthal correlations in hard processes, which are among the most interesting and least studied observables in QCD. Resummation and NP corrections are both quite large. A detailed experimental analysis (yet missing) would therefore be important in order to test our knowledge of QCD dynamics and confinement effects in multi-jet ensembles.

Acknowledgments

We are grateful to Yuri Dokshitzer for helpful discussions and suggestions, and to Giulia Zanderighi and Gavin Salam for support in the numerical analysis.

A. Elementary partonic cross-sections

For the elementary process (2.2) we may write the parton momenta P_1, P_2 as

$$\begin{aligned} P_1 &= \frac{Q}{2x}(1, 0, 0, -1), \quad P_2 = \frac{Q}{2}(z_0, 0, T_M, z_3), \\ z_0 &= \xi + \frac{(1-\xi)(1-x)}{x}, \quad z_3 = \xi - \frac{(1-\xi)(1-x)}{x}, \end{aligned} \quad (\text{A.1})$$

in terms of the variables in (2.3). Distinguishing P_2 and P_3 according to (2.5), the variable ξ is given in terms of T_M by

$$\xi = \frac{1}{2} \left[1 - \sqrt{1 - \frac{xT_M^2}{1-x}} \right], \quad (\text{A.2})$$

and in terms of y_2 by

$$\begin{aligned} \xi &= \frac{1-x}{2(2x-1)} \left[\sqrt{1 + \frac{4x(2x-1)y_2}{(1-x)^2}} - 1 \right], \quad \begin{cases} 0 < x < \frac{3}{4}, & 0 < y_2 < \frac{1}{4x} \\ \frac{3}{4} < x < 1, & 0 < y_2 < \frac{2(1-x)^2}{x(2x-1)} \end{cases} \\ \xi &= \frac{x^2 y_2 - (1-x)^2}{(2x-1)(1-x+xy_2)}, \quad \frac{3}{4} < x < 1, \quad \frac{2(1-x)^2}{x(2x-1)} < y_2 < \frac{1-x}{x} \end{aligned} \quad (\text{A.3})$$

The phase-space in terms of the variables (x, ξ) then becomes:

$$\begin{aligned} x_B < x < x_M, \quad x_M &= \begin{cases} \frac{1}{1+y_-}, & y_- < 1/3 \\ \frac{1}{4y_-}, & y_- > 1/3 \end{cases}, \\ \xi_- < \xi < \xi_+, \quad \xi_- &= \xi(x, y_-), \quad \xi_+ = \begin{cases} \xi(x, y_+), & x < \frac{1}{4y_+} \\ \frac{1}{2}, & x > \frac{1}{4y_+} \end{cases}. \end{aligned} \quad (\text{A.4})$$

We consider now the nature of the involved hard primary partons. We identify the incoming parton of momentum P_1 by the index $\tau = q, \bar{q}, g$. Since (2.5) distinguishes P_2 from P_3 , in order to completely fix the configurations of the three primary partons, we need to give an additional index $\delta = 1, 2, 3$ identifying the gluon. Therefore the primary partons with momenta $\{P_1, P_2, P_3\}$ are in the following five configurations

$$\begin{aligned} \tau = g, \delta = 1 &\rightarrow \{gq\bar{q}\}, \quad \text{or} \quad \{g\bar{q}q\} \\ \tau = q, \delta = 2 &\rightarrow \{qqq\}, \\ \tau = \bar{q}, \delta = 2 &\rightarrow \{\bar{q}g\bar{q}\}, \\ \tau = q, \delta = 3 &\rightarrow \{qqg\}, \\ \tau = \bar{q}, \delta = 3 &\rightarrow \{\bar{q}\bar{q}g\}. \end{aligned} \quad (\text{A.5})$$

Next we give the corresponding five elementary distributions $d\hat{\sigma}_{\tau,\delta,f}$, with f the fermion flavours. Since we consider only diagrams with the exchange of a single photon or Z_0 , the individual partonic cross-sections may be decomposed according to:

$$\frac{d\hat{\sigma}_{\tau,\delta,f}}{dx d\xi dQ^2} = \frac{\alpha^2 \alpha_s}{Q^4} \left\{ C^f(Q^2) \left[(2 - 2y + y^2) C_T^{\tau,\delta}(x, \xi) + 2(1 - y) C_L^{\tau,\delta}(x, \xi) \right] + D^f(Q^2) y(2 - y) C_3^{\tau,\delta}(x, \xi) \right\}, \quad (\text{A.6})$$

into transverse, longitudinal and parity-violating terms. Here y is defined by

$$y = \frac{(Pq)}{(PE_e)} = \frac{Q^2}{x_B s}, \quad (\text{A.7})$$

where P_e is the momentum of the incident electron, and s is the centre-of-mass energy squared of the collision (we neglect the proton mass). The flavour-dependent functions $C^f(Q^2)$ and $D^f(Q^2)$ show how the γ and Z exchange diagrams combine:

$$\begin{aligned} C^f(Q^2) &= e_f^2 - \frac{2e_f V_f V_e}{\sin^2 2\theta_W} \left(\frac{Q^2}{Q^2 + M^2} \right) + \frac{(V_f^2 + A_f^2)(V_e^2 + A_e^2)}{\sin^4 2\theta_W} \left(\frac{Q^2}{Q^2 + M^2} \right)^2, \\ D^f(Q^2) &= -\frac{2e_f A_q A_e}{\sin^2 2\theta_W} \left(\frac{Q^2}{Q^2 + M^2} \right) + \frac{4V_f A_f V_e A_e}{\sin^4 2\theta_W} \left(\frac{Q^2}{Q^2 + M^2} \right)^2. \end{aligned} \quad (\text{A.8})$$

The functions $C_{T/L/3}^{\tau,\delta}(x, \xi)$ are the one loop QCD elementary square matrix elements for the hard vertex (there is no contribution of order $\mathcal{O}(\alpha_s^0)$ since we require transverse jets). We have [21]

$$\begin{aligned} C_T^{q,3} &= C_F \left[\frac{x^2 + \xi^2}{(1-x)(1-\xi)} + 2(1+x\xi) \right], & C_T^{g,1} &= [x^2 + (1-x)^2] \frac{\xi^2 + (1-\xi)^2}{\xi(1-\xi)}, \\ C_L^{q,3} &= C_F \cdot 4x\xi, & C_L^{g,1} &= 8x(1-x), \\ C_3^{q,3} &= C_F \left[\frac{x^2 + \xi^2}{(1-x)(1-\xi)} + 2(x+\xi) \right], & C_3^{g,1} &= 0, \\ C_{T/L/3}^{q,2}(x, \xi) &= C_{T/L/3}^{q,3}(x, 1-\xi), & C_{T/L}^{\bar{q},\delta}(x, \xi) &= C_{T/L}^{q,\delta}(x, \xi), & C_3^{\bar{q},\delta}(x, \xi) &= -C_3^{q,\delta}(x, \xi). \end{aligned} \quad (\text{A.9})$$

If we consider only photon exchange the index τ is redundant, and the relevant elementary distributions $d\hat{\sigma}_{\delta,f}^{(\gamma)}$ are

$$\begin{aligned} \frac{d\hat{\sigma}_{\delta,f}^{(\gamma)}}{dx d\xi dQ^2} &= \frac{\alpha^2 \alpha_s}{Q^4} e_f^2 \left[(2 - 2y + y^2) C_T^\delta(x, \xi) + 2(1 - y) C_L^\delta(x, \xi) \right], \\ C_T^3 &= C_F \left[\frac{x^2 + \xi^2}{(1-x)(1-\xi)} + 2(1+x\xi) \right], & C_T^1 &= [x^2 + (1-x)^2] \frac{\xi^2 + (1-\xi)^2}{\xi(1-\xi)}, \\ C_L^3 &= C_F \cdot 4x\xi, & C_L^1 &= 8x(1-x), & C_{T/L}^2(x, \xi) &= C_{T/L}^3(x, 1-\xi). \end{aligned} \quad (\text{A.10})$$

B. Observable decomposition

Here we decompose the observable $H(\chi)$, defined in (1.1), in the case where we have two hard outgoing partons p_2 and p_3 accompanied by soft radiation k_i . Replacing the sum over hadrons in (1.1) by a sum over partons, and neglecting terms of $\mathcal{O}(k_i^2/Q^2)$, we obtain

$$H(\chi) = \frac{p_{t2}^2 + p_{t3}^2}{Q^2} \delta(\chi - \pi) + 2 \frac{p_{t2} p_{t3}}{Q^2} \delta(\chi - \chi_{23}) \\ + 2 \sum_i \frac{p_{t2} k_{ti}}{Q^2} \delta(\chi - \chi_{2i}) + 2 \sum_i \frac{p_{t3} k_{ti}}{Q^2} \delta(\chi - \chi_{3i}), \quad (\text{B.1})$$

with $\chi_{ab} = \pi - |\phi_{ab}|$.

In order to perform the calculation, we must introduce the definition of the event plane as the plane formed by the incoming proton direction \vec{n}_P in the Breit frame and the unit vector \vec{n}_M which enters the definition of thrust major

$$T_M = \max_{\vec{n}_M} \frac{1}{Q} \sum_h |\vec{p}_h \cdot \vec{n}_M|, \quad \vec{n}_M \cdot \vec{n}_P = 0. \quad (\text{B.2})$$

For dijet events with transverse momentum $P_t \sim Q$ we have $T_M = \mathcal{O}(1)$. Fixing the event plane as the yz plane, let the transverse momentum components of the outgoing partons be

$$\vec{p}_{t2} = P_t(\epsilon_1, 1 - \epsilon_2), \quad \vec{p}_{t3} = -P_t(\epsilon_3, 1 - \epsilon_4), \quad \vec{k}_{ti} = (k_{xi}, k_{yi}) = k_{ti}(\sin \phi_i, \cos \phi_i), \quad (\text{B.3})$$

with $P_t = \frac{1}{2}QT_M$. Conservation of momentum gives

$$\phi_x = \epsilon_3 - \epsilon_1 = \sum_i \frac{k_{xi}}{P_t}, \quad \epsilon_2 - \epsilon_4 = \sum_i \frac{k_{yi}}{P_t}, \quad (\text{B.4})$$

while the definition (B.2) of T_M gives

$$\epsilon_1 + \epsilon_3 = - \sum_i \frac{k_{xi}}{P_t} [\theta(k_{yi}) - \theta(-k_{yi})], \quad \epsilon_2 + \epsilon_4 = \sum_i \frac{|k_{yi}|}{P_t}. \quad (\text{B.5})$$

Thus

$$\epsilon_1 = - \sum_i \frac{k_{xi}}{P_t} \theta(k_{yi}) \quad \epsilon_2 = \sum_i \frac{k_{yi}}{P_t} \theta(k_{yi}) \\ \epsilon_3 = \sum_i \frac{k_{xi}}{P_t} \theta(-k_{yi}) \quad \epsilon_4 = - \sum_i \frac{k_{yi}}{P_t} \theta(-k_{yi}). \quad (\text{B.6})$$

Expanding up to terms linear in the soft momenta, we get

$$\chi_{23} = |\epsilon_3 - \epsilon_1| \quad \chi_{2i} = |\pi + \epsilon_1 - \phi_i| \quad \chi_{3i} = |\phi_i - \epsilon_3| \\ p_{t2} = P_t(1 - \epsilon_2) \quad p_{t3} = P_t(1 - \epsilon_4) \quad (\text{B.7})$$

Hence the observable $H(\chi)$ is given by

$$H(\chi) = \frac{2P_t^2}{Q^2} (1 - \epsilon_2 - \epsilon_4) [\delta(\chi - |\epsilon_3 - \epsilon_1|) + \delta(\chi - \pi)] \\ + \frac{2P_t}{Q^2} \sum_i k_{ti} [\delta(\chi - |\pi + \epsilon_1 - \phi_i|) + \delta(\chi - |\phi_i - \epsilon_3|)] . \quad (\text{B.8})$$

The first term is generated by the two hard partons, but has contributions both from the underlying hard momenta and from the soft parton recoil. The second term is the direct contribution from soft radiation.

Let us therefore take the recoil contribution from the first term (that proportional to $\epsilon_2 + \epsilon_4$) and add it to the soft term:

$$H(\chi) = \frac{2P_t^2}{Q^2} [\delta(\chi - |\epsilon_3 - \epsilon_1|) + \delta(\chi - \pi)] + \frac{2P_t}{Q^2} \sum_i k_{ti} \left[\delta(\chi - |\pi + \epsilon_1 - \phi_i|) \right. \\ \left. + \delta(\chi - |\phi_i - \epsilon_3|) - |\cos \phi_i| \delta(\chi - |\epsilon_3 - \epsilon_1|) - |\cos \phi_i| \delta(\chi - \pi) \right] . \quad (\text{B.9})$$

Note the cancellation of collinear singularities: when k_i is collinear to p_1 we have $\phi_i = \epsilon_1$, which generates cancellation between the second and third delta-functions in the soft term above, and between the first and fourth. (We have $\cos \phi_i = 1$ to this accuracy.) Similarly, when k_i is collinear to p_2 we have $\phi_i = \pi + \epsilon_3$, which generates cancellation between the first and third delta-functions, and between the second and fourth. (Now we have $\cos \phi_i = -1$.)

The above is valid for all χ up to $\chi = \pi$, but we are only interested in small χ for the resummation and leading power correction, with larger values of χ given by matching with the fixed order calculation. For small χ , we may write

$$H(\chi) \simeq \frac{2P_t^2}{Q^2} \delta(\chi - |\phi_x|) + \frac{2P_t}{Q^2} \sum_i k_{ti} \left[\delta(\chi - |\bar{\phi}_i - \phi_x|) - |\cos \bar{\phi}_i| \delta(\chi - |\phi_x|) \right] , \quad (\text{B.10})$$

where instead of ϕ_i we now use $\bar{\phi}_i$, the azimuthal angle between k_i and either the hard parton p_2 or p_3 :

$$\bar{\phi}_i = \begin{cases} \phi_{i2} = \phi_i - \epsilon_1 & \text{for } k_i \text{ near } p_2, \\ \phi_{3i} = \pi - \phi_i + \epsilon_3 & \text{for } k_i \text{ near } p_3. \end{cases} \quad (\text{B.11})$$

The cancellation of the collinear singularity is still manifest as we take $\bar{\phi}_i \rightarrow 0$.

C. DL approximation

Here we give an instructive simplified study of the behaviour of the small and large- b contributions to the distribution $\mathcal{I}(\chi)$. We use the DL radiation factor evaluated at

$P_t = \frac{1}{2}Q$, with a fixed value of the running coupling ($\alpha_s = 0.119$) and without parton distribution functions:

$$\mathcal{F}_{\text{DL}}(b) = e^{-R_{\text{DL}}(b)}, \quad R_{\text{DL}}(b) = \frac{\alpha_s C_T}{\pi} \ln^2(\bar{b} P_t), \quad \bar{b} = b e^{\gamma_E}. \quad (\text{C.1})$$

We separate the b -integral into a soft and hard contribution as indicated in equation (4.5), and discuss each contribution in turn.

C.1 Large b (soft) contribution

The large b or soft contribution is that arising from multiple gluon emissions with all $|k_x| < \chi P_t$, whose cumulative effect is a hard parton recoil of χP_t . Thus we expect to see in this contribution the usual Sudakov behaviour. We obtain

$$\begin{aligned} \mathcal{I}^{(+)}(\chi) &= \frac{d}{d\chi} \int_{\frac{1}{\bar{\chi} P_t}}^{\infty} \frac{db}{\pi b} \sin(P_t b \chi) e^{-R_{\text{DL}}(b)} \\ &\approx \frac{d}{d\chi} \cdot e^{-R_{\text{DL}}(\frac{1}{\bar{\chi} P_t})} \left[\frac{e^{-\gamma_E R'} \sec \frac{\pi}{2} R'}{2\Gamma(1+R')} - \frac{1}{\pi} \sum_{n=0}^{\infty} \frac{(-1)^n}{(2n+1)!} \frac{e^{-(2n+1)\gamma_E}}{2n+1-R'} \right], \end{aligned} \quad (\text{C.2})$$

where the function R' is

$$R' = \frac{2\alpha_s C_T}{\pi} \ln \frac{1}{\chi}, \quad (\text{C.3})$$

and the quantity in brackets is a SL function which equals $\frac{1}{2}$ at DL level. The result is well-defined and convergent for all R' , since the poles from the sec function are cancelled explicitly by the second term in the brackets. (If however we attempt the same procedure on the integral over the whole b range, we obtain only the first term, which diverges at $R' = 1$.)

The difference between the approximation and the exact value of the integral is formally beyond SL and is compensated for by the matching with fixed order. The Sudakov behaviour is clearly seen, along with the peak at $R' \approx 1$ (see figure 3).

C.2 Small b (hard) contribution

The small b or hard piece is that arising from two or more hard gluon emissions, with $|k_x| > \chi P_t$, but which combine with opposite signs to give the hard parton recoil of only χP_t . We can expand in powers of χ :

$$\begin{aligned} \mathcal{I}^{(-)}(\chi) &= \frac{d}{d\chi} \int_0^{\frac{1}{\bar{\chi} P_t}} \frac{db}{\pi b} \sin(P_t b \chi) e^{-R_{\text{DL}}(b)} \\ &= \frac{1}{\pi} \frac{d}{d\chi} \sum_{n=0}^{\infty} \frac{(-1)^n (\chi P_t)^{2n+1}}{(2n+1)!} \int_0^{\frac{1}{\bar{\chi} P_t}} db b^{2n} e^{-R_{\text{DL}}(b)}, \end{aligned} \quad (\text{C.4})$$

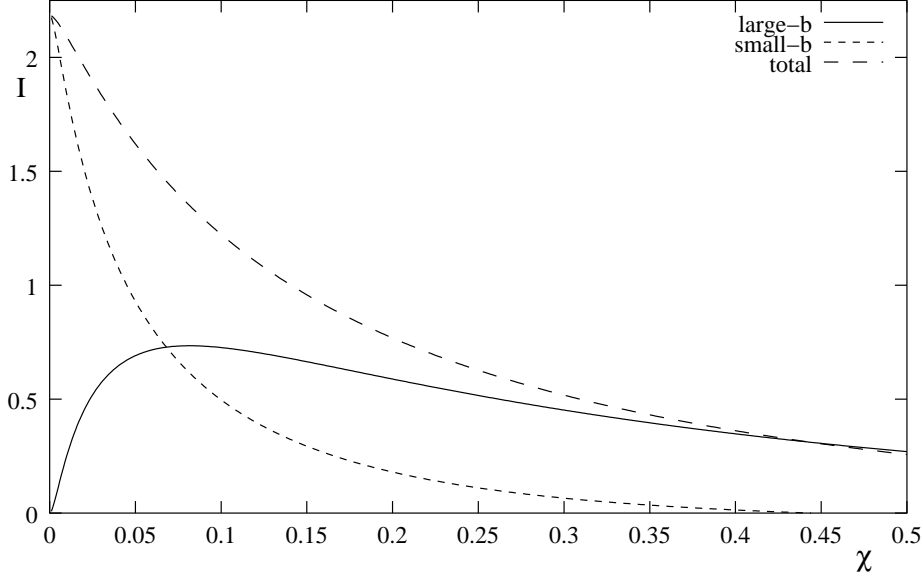


Figure 3: Hard, soft and total contributions to $\mathcal{I}(\chi)$ in the DL approximation for the azimuthal correlation.

and then integrate to give

$$\mathcal{I}^{(-)}(\chi) = \frac{1}{\pi} \frac{d}{d\chi} \sum_{n=0}^{\infty} \frac{(-1)^n (\chi e^{-\gamma_E})^{2n+1}}{(2n+1)!} \frac{e^{\frac{(2n+1)^2}{2a}}}{\sqrt{a}} \Phi \left(\sqrt{a} \ln \frac{1}{\chi} - \frac{2n+1}{\sqrt{a}} \right), \quad (\text{C.5})$$

where the quantity a and the function $\Phi(x)$ are

$$a = \frac{2\alpha_s C_T}{\pi}, \quad \Phi(x) = \int_{-\infty}^x dt e^{-\frac{1}{2}t^2}. \quad (\text{C.6})$$

The series is rapidly convergent since as n increases the argument of the Φ function becomes more negative. For this contribution there is no Sudakov behaviour, but rather at $\chi = 0$ the distribution increases to a constant that behaves as $1/\sqrt{\alpha_s}$.

In figure 3 are plotted the two contributions to \mathcal{I} as well as the total. Notice that at very small χ (i.e. with $R' > 1$) the soft radiation is suppressed and the distribution is due to hard emission. Soft radiation contributes around and above the Sudakov peak at $R' = 1$.

C.3 Comparison with EEC

The case of energy-energy correlation in e^+e^- is similar to the above, except that instead of C_T the total colour charge of the hard partons is $2C_F$, and the integration measure is substituted according to

$$\frac{db}{\pi b} \sin(P_t b \chi) \longrightarrow Q \chi db J_1 \left(\frac{Q}{2} b \chi \right). \quad (\text{C.7})$$

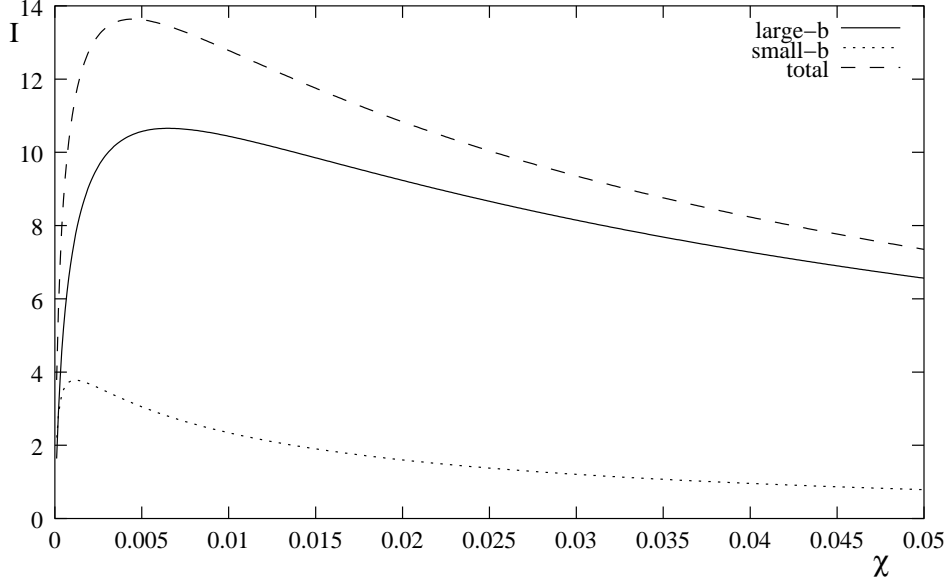


Figure 4: Hard, soft and total contributions to $\mathcal{I}(\chi)$ in the DL approximation for the EEC distribution.

In particular the 2-dimensional phase-space ensures that the distribution peaks and falls linearly to zero, while the fact that the SL approximation is valid up to $R' = 2$ means that it is a good approximation for in the region of the peak, up to matching with fixed order.

In figure 4 are plotted large and small- b contributions and the total for this distribution. The large- b contribution dominates until well below the peak. This very much simplified study shows the qualitative behaviour of the distribution in b -space, and gives a helpful insight into the physics of the azimuthal correlation.

D. Soft contribution

In this appendix we study the perturbative and non-perturbative contributions to the quantity $B_\delta(b)$ given in (3.13). We consider each dipole separately.

D.1 Dipoles 12 and 13

Consider

$$B_{12}(b) = \int \frac{d^3k}{\pi\omega} w_{12}(k) \frac{k_t}{P_t} [\cos(P_t b \bar{\phi}) - |\cos \bar{\phi}|] . \quad (\text{D.1})$$

Denoting by p_1^*, p_2^* and k^* the momenta in this system, we introduce the Sudakov decomposition

$$p_2^* = \frac{Q_{ab}}{2}(1, 0, 0, 1), \quad p_1^* = \frac{Q_{ab}}{2}(1, 0, 0, -1), \quad k^* = \alpha p_2^* + \beta p_1^* + \kappa, \quad (\text{D.2})$$

where the scale $Q_{12}^2 = 2(p_1 p_2)$. Here the two-dimensional vector $\vec{\kappa} = (\kappa_x, \kappa_y)$ is the transverse momentum orthogonal to the 12-dipole momenta ($\kappa^2 = k_{12,t}^2$). We have then

$$w_{12}(k) = \frac{\alpha_s(\kappa^2)}{\pi \kappa^2}, \quad \frac{d^3 k}{\pi \omega} = \frac{d^2 \kappa}{\pi} \frac{d\alpha}{\alpha}, \quad \alpha > \frac{\kappa^2}{Q_{12}^2}. \quad (\text{D.3})$$

We must also express the Breit-frame components of k in terms of these variables. The Sudakov variables α and β are Lorentz invariant, while the two-component vector $\vec{\kappa}$ transforms into a 4-vector with components

$$\kappa_0^{\text{Breit}} = \frac{P_t}{Q\xi} \kappa_y, \quad \kappa_x^{\text{Breit}} = \kappa_x, \quad \kappa_y^{\text{Breit}} = \kappa_y, \quad \kappa_z^{\text{Breit}} = -\frac{P_t}{Q\xi} \kappa_y. \quad (\text{D.4})$$

Thus the transverse momentum components of k in the Breit frame are

$$k_x = \kappa_x, \quad k_y = \alpha P_t + \kappa_y. \quad (\text{D.5})$$

We take $\bar{\phi}$ as the azimuthal angle between p_2 and k — this neglects the contribution from k near to p_3 , which contributes beyond SL and so is included by matching with the fixed order result. Therefore

$$\cot \bar{\phi} = \frac{k_y}{k_x} = \frac{\kappa_y}{\kappa_x} + \frac{\alpha P_t}{\kappa_x} = \cot \phi + \frac{\alpha P_t}{\kappa} \csc \phi, \quad (\text{D.6})$$

and the 12-dipole contribution is

$$B_{12}(b) = \int \frac{d\kappa^2}{\kappa^2} \frac{d\phi}{2\pi} \frac{d\alpha}{\alpha} \frac{\alpha_s(\kappa)}{\pi} \cdot \frac{\kappa \sin \phi}{P_t \sin \bar{\phi}} [\cos(P_t b \bar{\phi}) - |\cos \bar{\phi}|]. \quad (\text{D.7})$$

Changing integration variable from α to $\bar{\phi}$ gives

$$B_{12}(b) = \frac{2}{\pi P_t} \int d\kappa \alpha_s(\kappa) \int_0^\pi \frac{d\phi}{\pi} \sin^2 \phi \int_{\bar{\phi}_m}^{\bar{\phi}_M} \frac{d\bar{\phi}}{\sin(\phi - \bar{\phi})} \cdot \frac{\cos(P_t b \bar{\phi}) - |\cos \bar{\phi}|}{\sin^2 \bar{\phi}}, \quad (\text{D.8})$$

$$\cot \bar{\phi}_m = \cot \phi + \frac{P_t}{\kappa} \csc \phi, \quad \cot \bar{\phi}_M = \cot \phi + \frac{P_t \kappa}{Q_{12}^2} \csc \phi,$$

which is clearly beyond SL, since both the soft logarithm ($\kappa \rightarrow 0$) and the collinear logarithm ($\bar{\phi} \rightarrow 0$) are cancelled. The 13-dipole is treated similarly.

D.2 Dipole 23

The 23-dipole is analysed along the same lines as the 12, except that there are some minor differences. Again we introduce the Sudakov decomposition

$$p_2^* = \frac{Q_{23}}{2}(1, 0, 0, 1), \quad p_3^* = \frac{Q_{23}}{2}(1, 0, 0, -1), \quad k^* = \alpha p_2^* + \beta p_3^* + \kappa. \quad (\text{D.9})$$

We must again express the Breit-frame components of k in terms of these variables, but now the two-component vector $\vec{\kappa}$ transforms into a 4-vector with components

$$\kappa_0^{\text{Breit}} = \frac{P_t(2x-1)}{Q(1-x)}\kappa_y, \quad \kappa_x^{\text{Breit}} = \kappa_x, \quad \kappa_y^{\text{Breit}} = (1-2\xi)\kappa_y, \quad \kappa_z^{\text{Breit}} = \frac{P_t}{Q(1-x)}\kappa_y. \quad (\text{D.10})$$

The transverse momentum components of k in the Breit frame are then

$$k_x = \kappa_x, \quad k_y = (\alpha - \beta)P_t + (1 - 2\xi)\kappa_y. \quad (\text{D.11})$$

We take $\bar{\phi}$ as the azimuthal angle between p_2 and k in the region where $\alpha > \beta$, and as the angle between p_3 and k when $\alpha < \beta$. The neglected contributions are beyond SL and so are included by matching with the fixed order result. We take each hemisphere separately: in the right hemisphere ($\alpha > \beta$)

$$\cot \bar{\phi} = (1 - 2\xi) \cot \phi + \frac{(\alpha - \beta)P_t}{\kappa} \csc \phi, \quad (\text{D.12})$$

and the 23-dipole right hemisphere contribution is

$$B_{23}^R(b) = \int_{\alpha > \beta} \frac{d\kappa^2}{\kappa^2} \frac{d\phi}{2\pi} \frac{d\alpha}{\alpha} \frac{\alpha_s(\kappa)}{\pi} \cdot \frac{\kappa \sin \phi}{P_t \sin \bar{\phi}} [\cos(P_t b \bar{\phi}) - |\cos \bar{\phi}|]. \quad (\text{D.13})$$

Changing integration variable from α to $\bar{\phi}$ gives

$$\begin{aligned} B_{23}^R(b) &= \frac{2}{\pi P_t} \int d\kappa \alpha_s(\kappa) \int_0^\pi \frac{d\phi}{\pi} \sin^2 \phi \int_{\bar{\phi}_m}^{\bar{\phi}_M} \frac{d\bar{\phi}}{\sqrt{f(\phi, \bar{\phi})}} \cdot \frac{\cos(P_t b \bar{\phi}) - |\cos \bar{\phi}|}{\sin^2 \bar{\phi}}, \\ f(\phi, \bar{\phi}) &= [\sin \phi \cos \bar{\phi} - (1 - 2\xi) \cos \phi \sin \bar{\phi}]^2 + 4 \frac{P_t^2}{Q_{23}^2} \sin^2 \bar{\phi} \\ \cot \bar{\phi}_m &= (1 - 2\xi) \cot \phi + \frac{P_t}{\kappa} \csc \phi, \quad \cot \bar{\phi}_M = (1 - 2\xi) \cot \phi, \end{aligned} \quad (\text{D.14})$$

which is clearly beyond SL, since both the soft logarithm ($\kappa \rightarrow 0$) and the collinear logarithm ($\bar{\phi} \rightarrow 0$) are cancelled. The left hemisphere is treated similarly.

D.3 NP contribution

We calculate the NP contribution using the standard procedure, see [5].

Applying this to equation (D.8) gives the NP contribution to B_{12} as

$$\begin{aligned} \delta B_{12}(b) &= \frac{\mathcal{M}}{\pi} \int dm^2 \delta\alpha_{\text{eff}}(m^2) \frac{-d}{dm^2} \int_0^\infty \frac{d\kappa^2}{P_t \sqrt{\kappa^2 + m^2}} \int_0^\pi \frac{d\phi}{\pi} \sin^2 \phi \\ &\quad \times \int_{\bar{\phi}_m}^{\bar{\phi}_M} \frac{d\bar{\phi}}{\sin(\phi - \bar{\phi})} \cdot \frac{\cos(P_t b \bar{\phi}) - |\cos \bar{\phi}|}{\sin^2 \bar{\phi}}, \\ \cot \bar{\phi}_m &= \cot \phi + \frac{P_t}{\sqrt{\kappa^2 + m^2}} \csc \phi, \quad \cot \bar{\phi}_M = \cot \phi + \frac{P_t \sqrt{\kappa^2 + m^2}}{Q_{12}^2} \csc \phi. \end{aligned} \quad (\text{D.15})$$

Here \mathcal{M} is the Milan factor [16] which accounts for the non fully inclusive nature of the observable.

Doing the m -derivative and κ -integral gives

$$\begin{aligned}\delta B_{12}(b) &= \frac{2\mathcal{M}}{\pi P_t} \int dm \delta\alpha_{\text{eff}}(m^2) \int_0^\pi \frac{d\phi}{\pi} \sin^2 \phi \int_{\bar{\phi}_m}^{\bar{\phi}_M} \frac{d\bar{\phi}}{\sin(\phi - \bar{\phi})} \cdot \frac{\cos(P_t b \bar{\phi}) - |\cos \bar{\phi}|}{\sin^2 \bar{\phi}}, \\ \cot \bar{\phi}_m &= \cot \phi + \frac{P_t}{m} \csc \phi, \quad \cot \bar{\phi}_M = \cot \phi + \frac{P_t m}{Q_{12}^2} \csc \phi.\end{aligned}\tag{D.16}$$

We wish to find the leading term in the expansion of this integral in the range $m \ll b^{-1} \ll P_t$. Writing $\bar{\phi} = u/(bP_t)$ and expanding the integrand yields

$$\begin{aligned}\delta B_{12}(b) &= \frac{2\mathcal{M}}{\pi P_t} \int dm \delta\alpha_{\text{eff}}(m^2) \int_0^\pi \frac{d\phi}{\pi} \sin \phi \int_0^\infty b P_t du \frac{\cos u - 1}{u^2} + \dots \\ &= -b \cdot \lambda^{\text{NP}} + \dots \quad \lambda^{\text{NP}} = \frac{2\mathcal{M}}{\pi} \int dm \delta\alpha_{\text{eff}}(m^2),\end{aligned}\tag{D.17}$$

where the dots involves terms which are of higher order in b . The 13-dipole gives an identical result.

The same procedure applied to equation (D.14) gives the NP contribution to B_{23}^R as

$$\begin{aligned}\delta B_{23}^R(b) &= \frac{\mathcal{M}}{\pi} \int dm^2 \delta\alpha_{\text{eff}}(m^2) \frac{-d}{dm^2} \int_0^\infty \frac{d\kappa^2}{P_t \sqrt{\kappa^2 + m^2}} \int_0^\pi \frac{d\phi}{\pi} \sin^2 \phi \\ &\quad \times \int_{\bar{\phi}_m}^{\bar{\phi}_M} \frac{d\bar{\phi}}{\sqrt{f(\phi, \bar{\phi})}} \cdot \frac{\cos(P_t b \bar{\phi}) - |\cos \bar{\phi}|}{\sin^2 \bar{\phi}}, \\ \cot \bar{\phi}_m &= (1 - 2\xi) \cot \phi + \frac{P_t}{\sqrt{\kappa^2 + m^2}} \csc \phi, \quad \cot \bar{\phi}_M = (1 - 2\xi) \cot \phi.\end{aligned}\tag{D.18}$$

Doing the m -derivative and κ -integral gives

$$\begin{aligned}\delta B_{23}^R(b) &= \frac{2\mathcal{M}}{\pi P_t} \int dm \delta\alpha_{\text{eff}}(m^2) \int_0^\pi \frac{d\phi}{\pi} \sin^2 \phi \int_{\bar{\phi}_m}^{\bar{\phi}_M} \frac{d\bar{\phi}}{\sqrt{f(\phi, \bar{\phi})}} \cdot \frac{\cos(P_t b \bar{\phi}) - |\cos \bar{\phi}|}{\sin^2 \bar{\phi}}, \\ \cot \bar{\phi}_m &= (1 - 2\xi) \cot \phi + \frac{P_t}{m} \csc \phi, \quad \cot \bar{\phi}_M = (1 - 2\xi) \cot \phi.\end{aligned}\tag{D.19}$$

We wish to find the leading term in the expansion of this integral in the range $m \ll b^{-1} \ll P_t$. Writing $\bar{\phi} = u/(bP_t)$ and expanding the integrand yields

$$\begin{aligned}\delta B_{23}^R(b) &= \frac{2\mathcal{M}}{\pi P_t} \int dm \delta\alpha_{\text{eff}}(m^2) \int_0^\pi \frac{d\phi}{\pi} \sin \phi \int_0^\infty b P_t du \frac{\cos u - 1}{u^2} + \dots \\ &= -b \cdot \lambda^{\text{NP}} + \dots\end{aligned}\tag{D.20}$$

where, as before, the terms in the dots are of order b^2 . The left hemisphere gives an identical result, and so the total is

$$\delta B_{23}(b) = -2b \cdot \lambda^{\text{NP}} + \dots \quad (\text{D.21})$$

Combining the three dipoles then gives the leading non-perturbative contribution

$$\delta B_\delta(b) = - \left(C_2^{(\delta)} + C_3^{(\delta)} \right) b \cdot \lambda^{\text{NP}}. \quad (\text{D.22})$$

The complete treatment of this correction requires the definition of the coupling in the infra-red region (this will be done by the dispersive method [5]), the analysis of contributions which are non fully inclusive, leading to the Milan factor [16], and of the merging PT and NP contributions to the observable in a renormalon free manner. This can be done in the usual way and the NP parameter is given by

$$\lambda^{\text{NP}} \equiv \mathcal{M} \frac{4}{\pi^2} \mu_I \left\{ \alpha_0(\mu_I) - \bar{\alpha}_s - \beta_0 \frac{\bar{\alpha}_s^2}{2\pi} \left(\ln \frac{Q}{\mu_I} + \frac{K}{\beta_0} + 1 \right) \right\}, \quad (\text{D.23})$$

where

$$\bar{\alpha}_s \equiv \alpha_{\overline{\text{MS}}}(Q), \quad K \equiv C_A \left(\frac{67}{18} - \frac{\pi^2}{6} \right) - \frac{5}{9} n_f, \quad \beta_0 = \frac{11N_c}{3} - \frac{2n_f}{3}. \quad (\text{D.24})$$

The K factor accounts for the mismatch between the $\overline{\text{MS}}$ and the physical scheme [15] and $\alpha_0(\mu_I)$ is the integral of the running coupling over the infra-red region, see [5]. We have that, at two loops, λ^{NP} is independent of μ_I . Assuming universality of the coupling [5, 20] this NP parameter is the same as already measured in 2-jet observables. For instance, the shift for the $\tau = 1 - T$ distribution is

$$\frac{d\sigma}{d\tau}(\tau) = \frac{d\sigma^{\text{PT}}}{d\tau}(\tau - \Delta_\tau), \quad \Delta_\tau = C_F c_\tau \lambda^{\text{NP}}, \quad c_\tau = 2, \quad (\text{D.25})$$

where C_F enters due to the fact the 2-jet system is made of a quark-antiquark pair.

E. Estimates of $\langle b \rangle$ using 1-loop coupling

We consider using the 1-loop running coupling

$$\alpha_s(k) = \frac{2\pi}{\beta_0} \frac{1}{\ln(k/\Lambda)}. \quad (\text{E.1})$$

The DL function $r(\bar{b}, Q)$ defined in (4.1) then becomes

$$r(\bar{b}, Q) = \frac{4}{\beta_0} \left[\ln(Q/\Lambda) \ln \frac{\ln(2Q/\Lambda)}{\ln(2/\bar{b}\Lambda)} - \ln(\bar{b}Q) \right], \quad \bar{b} < \frac{2}{\Lambda}, \quad (\text{E.2})$$

and we impose $r(\bar{b}, Q) = \infty$ for $\bar{b} > \frac{2}{\Lambda}$. We also use parton density functions determined by the 1-loop evolution equation

$$\frac{\partial \mathcal{P}_N(k)}{\partial \ln k} = \frac{\alpha_s(k)}{\pi} \gamma_N \cdot \mathcal{P}_N(k) \quad (\text{E.3})$$

with γ_N the leading-order anomalous dimension matrix, and $\mathcal{P}_N(k)$ the moments of the parton density functions at scale k . This equation has solution

$$\mathcal{P}_N(k) = \left(\frac{\ln(k/\Lambda)}{\ln(Q/\Lambda)} \right)^{\frac{2}{\beta_0} \gamma_N} \cdot \mathcal{P}_N(Q) \quad (\text{E.4})$$

We define the integrals

$$I_n^{(\delta)}(N) = \int_0^\infty db b^n \mathcal{P}_N(2\bar{b}^{-1}) e^{-R_\delta(\bar{b})}, \quad \bar{b} = b e^{\gamma_E}, \quad (\text{E.5})$$

using the radiator given in (4.1). The choice of $2\bar{b}^{-1}$ rather than \bar{b}^{-1} as the factorisation scale is merely for convenience — the difference is beyond SL. Evaluation yields

$$I_n^{(\delta)}(N) = \left(\frac{2e^{-\gamma_E}}{\Lambda} \right)^n \left(\frac{1 + \frac{4}{\beta_0} C_T}{n + 1 + \frac{4}{\beta_0} C_T} \right)^{1 + \frac{2}{\beta_0} \gamma_N + \frac{4}{\beta_0} \sum_{a=1}^3 C_a^{(\delta)} \ln \frac{\zeta_a^{(\delta)} Q_a^{(\delta)}}{\Lambda}} \cdot I_0^{(\delta)}(N) \quad (\text{E.6})$$

with

$$\begin{aligned} I_0^{(\delta)} &= \frac{2e^{-\gamma_E}}{\Lambda} \left(\ln \frac{Q}{\Lambda} \right)^{-\frac{2}{\beta_0} \gamma_N} \frac{\Gamma \left(1 + \frac{2}{\beta_0} \gamma_N + \frac{4}{\beta_0} \sum_{a=1}^3 C_a^{(\delta)} \ln \frac{\zeta_a^{(\delta)} Q_a^{(\delta)}}{\Lambda} \right)}{\left(1 + \frac{4}{\beta_0} C_T \right)^{1 + \frac{2}{\beta_0} \gamma_N + \frac{4}{\beta_0} \sum_{a=1}^3 C_a^{(\delta)} \ln \frac{\zeta_a^{(\delta)} Q_a^{(\delta)}}{\Lambda}}} \\ &\times \prod_{a=1}^3 \left(\frac{2\zeta_a^{(\delta)} Q_a^{(\delta)}}{\Lambda} \right)^{\frac{4}{\beta_0} C_a^{(\delta)}} \prod_{a=1}^3 \left(\ln \frac{2\zeta_a^{(\delta)} Q_a^{(\delta)}}{\Lambda} \right)^{-\frac{4}{\beta_0} C_a^{(\delta)} \ln \frac{\zeta_a^{(\delta)} Q_a^{(\delta)}}{\Lambda}} \cdot \mathcal{P}_N(Q) \end{aligned} \quad (\text{E.7})$$

The average value of b is therefore, at fixed N ,

$$\langle b \rangle_N = \frac{I_1^{(\delta)}(N)}{I_0^{(\delta)}(N)} \sim \frac{a_\delta(N)}{\Lambda} \left(\frac{\Lambda}{Q} \right)^{\frac{4}{\beta_0} C_T \ln \frac{2 + \frac{4}{\beta_0} C_T}{1 + \frac{4}{\beta_0} C_T}} \quad (\text{E.8})$$

with a coefficient a_δ that depends on N . The exponent is N -independent and then we obtain the DL estimate in (4.19).

F. Formulæ for numerical analysis

In this appendix we report some analytical formulae needed to perform the numerical analysis described in section 5.

Within SL accuracy the PT radiator (4.1) can be written as

$$R_\delta(b) = C_T r_1(\bar{b}) - C_T \ln 2 r'(\bar{b}) + \sum_a C_a^{(\delta)} \ln \frac{Q_a^{(\delta)} \zeta_a^{(\delta)}}{Q} r_2(\bar{b}), \quad \bar{b} = b e^{\gamma_E}, \quad (\text{F.1})$$

where $Q_a^{(\delta)}$, $\zeta_a^{(\delta)}$ and $C_a^{(\delta)}$ are introduced in (4.2), while r_1, r_2 and r' are given by:

$$\begin{aligned} r_1(\bar{b}) &= \int_{1/\bar{b}}^Q \frac{dk}{k} \frac{2\alpha_s(k)}{\pi} \ln \frac{Q}{k} = -\frac{8\pi}{\beta_0^2 \bar{\alpha}_s} (\ell + \ln(1-\ell)) + \frac{4K}{\beta_0^2} \left(\ln(1-\ell) + \frac{\ell}{1-\ell} \right) \\ &\quad - \frac{4\beta_1}{\beta_0^3} \left(\frac{1}{2} \ln^2(1-\ell) + \frac{\ln(1-\ell) + \ell}{1-\ell} \right), \quad \ell = \frac{\bar{\alpha}_s}{2\pi} \beta_0 \ln \bar{b} Q, \\ r_2(\bar{b}) &= \int_{1/\bar{b}}^Q \frac{dk}{k} \frac{2\alpha_s(k)}{\pi} = -\frac{4}{\beta_0} \ln(1-\ell), \quad r'(\bar{b}) = \frac{2\alpha_s(\bar{b}^{-1})}{\pi} \ln \bar{b} Q = \frac{4}{\beta_0} \frac{\ell}{1-\ell}. \end{aligned} \quad (\text{F.2})$$

In the above expressions β_0 can be found in (D.24) and β_1 is given by:

$$\beta_1 = \frac{17C_A^2 - 5C_A n_f - 3C_F n_f}{3}. \quad (\text{F.3})$$

The coupling $\bar{\alpha}_s$ is in the $\overline{\text{MS}}$ scheme and the constant K relating the physical scheme [15] to the $\overline{\text{MS}}$ is defined in (D.24).

Actually (F.2) makes sense only for $\ell < 1$, so that, as usual (see [3]), we impose

$$e^{-R(b)} = 0, \quad \text{for } \bar{b} Q > \exp\left(\frac{2\pi}{\bar{\alpha}_s \beta_0}\right). \quad (\text{F.4})$$

We report also the expression for the coefficients G_{11} and c_1^{res} introduced in (5.2):

$$\begin{aligned} G_{11}(y_\pm) &= -\sigma^{-1}(y_\pm) \sum_\rho \int_{x_B}^{x_M} \frac{dx}{x} \int_{\xi_-}^{\xi_+} d\xi \left(\frac{d\hat{\sigma}_\rho}{dx d\xi dQ^2} \right) \frac{4P_t^2}{Q^2} \mathcal{P}_\rho\left(\frac{x_B}{x}, Q\right) \\ &\quad \cdot \left(4 \sum_a C_a^{(\delta)} \ln \frac{Q_a^{(\delta)} \zeta_a^{(\delta)}}{2P_t} + \frac{2\pi}{\alpha_s} \frac{\partial \ln \mathcal{P}_\rho}{\partial \ln Q} \right), \\ c_1^{\text{res}}(y_\pm) &= \sigma^{-1}(y_\pm) \sum_\rho \int_{x_B}^{x_M} \frac{dx}{x} \int_{\xi_-}^{\xi_+} d\xi \left(\frac{d\hat{\sigma}_\rho}{dx d\xi dQ^2} \right) \frac{4P_t^2}{Q^2} \mathcal{P}_\rho\left(\frac{x_B}{x}, Q\right) \\ &\quad \cdot \left(\ln \frac{P_t}{Q} \left(4 \sum_a C_a^{(\delta)} \ln \frac{Q_a^{(\delta)} \zeta_a^{(\delta)}}{2Q} + \frac{2\pi}{\alpha_s} \frac{\partial \ln \mathcal{P}_\rho}{\partial \ln Q} \right) - C_T \frac{\pi^2}{6} - 2C_T \ln^2 \frac{P_t}{Q} \right). \end{aligned} \quad (\text{F.5})$$

References

- [1] C.L. Basham, L.S. Brown, S.D. Ellis and S.T. Love, *Phys. Rev. Lett.* **41** (1978) 1585; *Phys. Rev.* **D 19** (1979) 2018;
J.C. Collins and D.E. Soper, *Nucl. Phys.* **B 193** (1981) 381, Erratum *ibid.* **213** (1983) 545; *ibid.* **197** (1982) 446; *Phys. Rev. Lett.* **48** (1982) 655;
J. Kodaira and L. Trentadue, *Phys. Lett.* **B 123** (1983) 335;
J.C. Collins and D.E. Soper, *Acta Phys. Polon.* **B 16** (1985) 1047; *Nucl. Phys.* **B 284** (1987) 253.
- [2] G. Parisi and R. Petronzio, *Nucl. Phys.* **B 154** (1979) 427.
- [3] Yu.L. Dokshitzer, G. Marchesini and B.R. Webber, *J. High Energy Phys.* **07** (1999) 012 [hep-ph/9905339].
- [4] S. Catani, Yu.L. Dokshitzer and B.R. Webber, *Phys. Lett.* **B 322** (1994) 263.
- [5] Yu.L. Dokshitzer, G. Marchesini and B.R. Webber, *Nucl. Phys.* **B 469** (1996) 93 [hep-ph/9512336].
- [6] A. Banfi, Yu.L. Dokshitzer, G. Marchesini and G. Zanderighi, *Phys. Lett.* **B 508** (2001) 269 [hep-ph/0010267]; *J. High Energy Phys.* **07** (2000) 002 [hep-ph/0004027]; *ibid.* **03** (2001) 007 [hep-ph/0101205]; *ibid.* **05** (2001) 040 [hep-ph/0104162].
- [7] A. Banfi, G. Marchesini, G. Smye and G. Zanderighi, *J. High Energy Phys.* **11** (2001) 066, [hep-ph/0111157].
- [8] PLUTO Collaboration: C. Berger et al., *Phys. Lett.* **B 99** (1980) 292;
OPAL Collaboration: P.D. Acton et al., *Zeit. Phys.* **C 59** (1993) 1;
SLD Collaboration: K. Abe et al. *Phys. Rev.* **D 51** (1995) 962.
- [9] J.F. Owens, *Phys. Rev.* **D 65** (2002) 034011 [hep-ph/0110036].
- [10] A. Banfi, G. Marchesini, G. Smye and G. Zanderighi, *J. High Energy Phys.* **08** (2001) 047 [hep-ph/0106278].
- [11] S. Catani, L. Trentadue, G. Turnock and B.R. Webber, *Nucl. Phys.* **B 407** (1993) 3;
S. Catani, G. Turnock and B.R. Webber, *Phys. Lett.* **B 295** (1992) 269;
S. Catani and B.R. Webber, *Phys. Lett.* **B 427** (1998) 377 [hep-ph/9801350];
Yu.L. Dokshitzer, A. Lucenti, G. Marchesini and G.P. Salam, *J. High Energy Phys.* **01** (1998) 011 [hep-ph/9801324].
- [12] V. Antonelli, M. Dasgupta and G.P. Salam, *J. High Energy Phys.* **02** (2000) 001 [hep-ph/9912488];
M. Dasgupta and G.P. Salam, hep-ph/0110213.
- [13] B.R. Webber, *Phys. Lett.* **B 339** (1994) 148 [hep-ph/9408222]; see also *Proc. Summer School on Hadronic Aspects of Collider Physics*, Zuoz, Switzerland, August 1994, ed. M.P. Locher (PSI, Villigen, 1994) [hep-ph/9411384];

- M. Beneke and V.M. Braun, *Nucl. Phys.* **B 454** (1995) 253 [hep-ph/9506452];
 Yu.L. Dokshitzer and B.R. Webber, *Phys. Lett.* **B 352** (1995) 451 [hep-ph/9504219];
 R. Akhouri and V.I. Zakharov, *Phys. Lett.* **B 357** (1995) 646 [hep-ph/9504248]; *Nucl. Phys.* **B 465** (1996) 295 [hep-ph/9507253];
 G.P. Korchemsky and G. Sterman, *Nucl. Phys.* **B 437** (1995) 415 [hep-ph/9411211];
 Yu.L. Dokshitzer, V.A. Khoze and S.I. Troyan, *Phys. Rev.* **D 53** (1996) 89 [hep-ph/9506425];
 P. Nason and B.R. Webber, *Phys. Lett.* **B 395** (1997) 355 [hep-ph/9612353];
 P. Nason and M.H. Seymour, *Nucl. Phys.* **B 454** (1995) 291 [hep-ph/9506317];
 Yu.L. Dokshitzer, G. Marchesini and B.R. Webber, *J. High Energy Phys.* **07** (1999) 012 [hep-ph/9905339];
 M. Beneke, *Phys. Rep.* **317** (1999) 1 [hep-ph/9807443];
 S.J. Brodsky, E. Gardi, G. Grunberg, J. Rathsmann, *Phys. Rev.* **D 63** (2001) 094017 [hep-ph/0002065];
 E. Gardi and J. Rathsmann, *Nucl. Phys.* **B 609** (2001) 123 [hep-ph/0103217].
- [14] Yu. L. Dokshitzer, D.I. Dyakonov and S.I. Troyan, *Phys. Rep.* **58** (1980) 270;
 A. Bassetto, M. Ciafaloni and G. Marchesini, *Phys. Rep.* **100** (1983) 201.
- [15] S. Catani, G. Marchesini and B.R. Webber, *Nucl. Phys.* **B 349** (1991) 635.
- [16] Yu.L. Dokshitzer, A. Lucenti, G. Marchesini and G.P. Salam, *Nucl. Phys.* **B 511** (1998) 396, [hep-ph/9707532], erratum *ibid.* **B593** (2001) 729; *J. High Energy Phys.* **05** (1998) 003 [hep-ph/9802381];
 M. Dasgupta and B.R. Webber *J. High Energy Phys.* **10** (1998) 001 [hep-ph/9809247];
 M. Dasgupta, L. Magnea and G. Smye, *J. High Energy Phys.* **11** (1999) 25 [hep-ph/9911316];
 G. Smye, *J. High Energy Phys.* **05** (2001) 005 [hep-ph/0101323].
- [17] S. Catani and M. Seymour, *Nucl. Phys.* **B 485** (1997) 291 [hep-ph/9605323].
- [18] D. Graudenz, hep-ph/9710244;
 E. Mirkes, D. Zeppenfeld, hep-ph/9706437;
 Z. Nagy, Z. Trocsanyi *Phys. Rev. Lett.* **87** (2001) 082001 [hep-ph/0104315].
- [19] A.D. Martin, R.G. Roberts, W.J. Stirling and R.S. Thorne, *Eur. Phys. J.* **C 14** (2000) 133 [hep-ph/9907231]; hep-ph/0110215.
- [20] G.P. Salam and G. Zanderighi, *Nucl. Phys.* **86 (Proc. Suppl.)** (2000) 430 [hep-ph/9909324].
- [21] K.H. Streng, T.F. Walsh and P.M. Zerwas, *Z. Physik* **C 2** (1979) 237;
 R.D. Peccei and R. Rückl, *Nucl. Phys.* **B 162** (1980) 125.